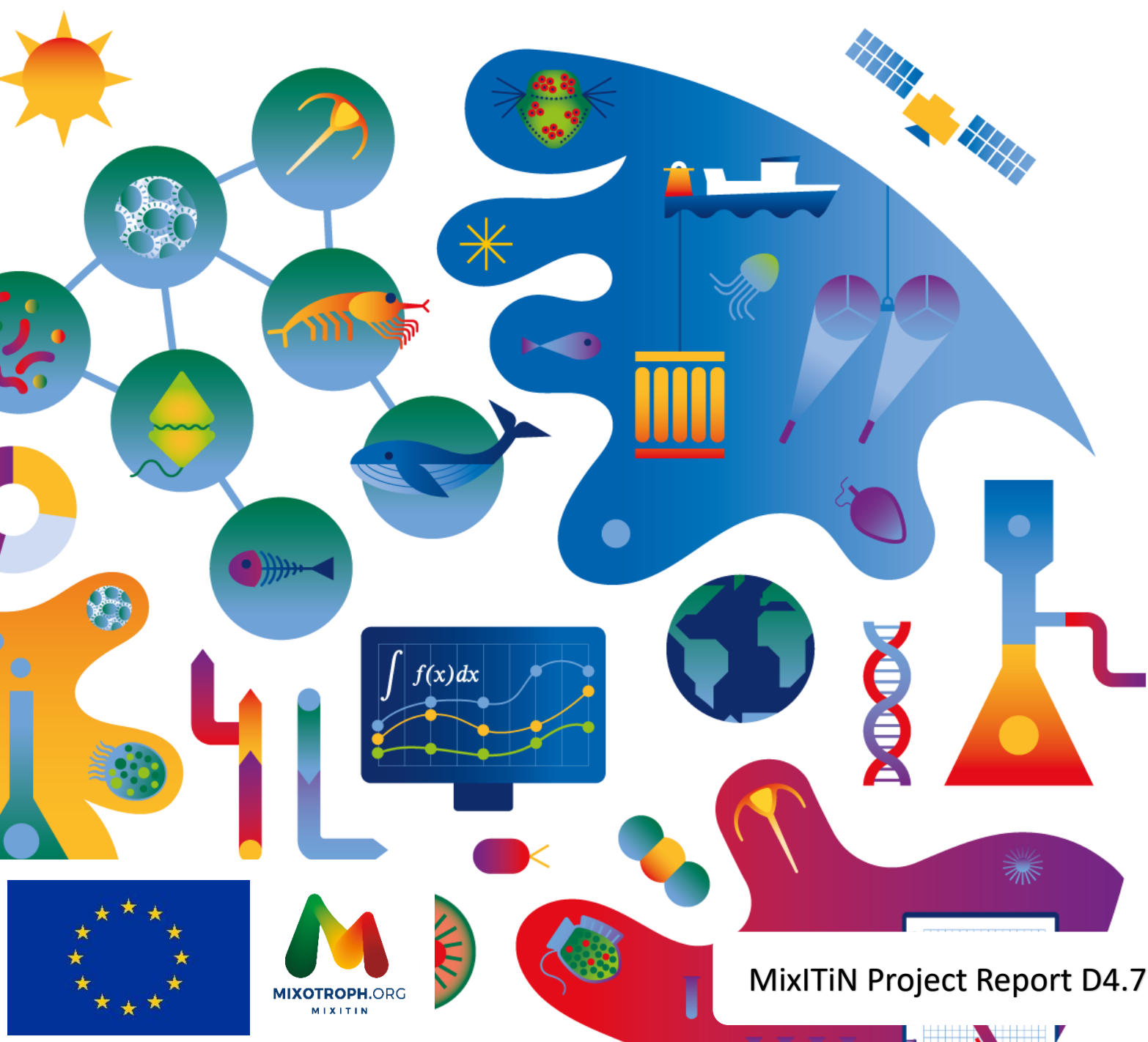


Seasonal Distribution Of Non-Constitutive Mixoplankton Across Arctic, Temperate and Mediterranean Coastal Waters



H2020-MSCA-ITN
Bringing marine ecology
into 21st century



Training next generation
marine ecologists in the
mixotroph paradigm

MixITiN

Project no. 766327

Seasonal Distribution Of Non-Constitutive Mixoplankton Across Arctic, Temperate And Mediterranean Coastal Waters

Aditee Mitra, Kevin J Flynn, Maira Maselli,
Per Juel Hansen, Nathalie Gypens, Jon Lapeyra Martin,
Filomena Romano, Paraskevi Pitta

Acknowledgements

*Project **MixITIN** has received funding from the European Union's Horizon 2020 research and innovation programme under the Marie Skłodowska-Curie grant agreement No 766327. This document reflects only the author's view; the REA and the European Commission are not responsible for any use that may be made of the information it contains.*

How to cite this work

Mitra A, Flynn KJ, Maselli M, Hansen PJ, Gypens N, Lapeyra Martin J, Romano F, Pitta P (2021) *Report of seasonal distribution of non-constitutive mixoplankton across Arctic, Temperate and Mediterranean coastal waters*. Publisher: Zenodo, <http://doi.org/10.5281/zenodo.5055707>

Copyright © 2021 Mitra, Flynn, Maselli, Hansen, Gypens, Martin, Romano and Pitta

This is an open-access article distributed under the terms of the [Creative Commons Attribution License](#) (CC BY). The use, distribution or reproduction in other forums is permitted, provided the original author(s) and the copyright owner(s) are credited and that the original publication on Zenodo is cited, in accordance with accepted academic practice. No use, distribution or reproduction is permitted which does not comply with these terms.

Updates

Please check for any updates in the latest version of this publication by visiting the url given in 'How to cite this work', above. If you note any errors, please contact the project co-ordinator. Thank you.

Project Co-ordinator contact

Aditee Mitra
School of Earth and Environmental Sciences
Cardiff University
Cardiff CF10 3AT
Wales, U.K.
Email: MitraA2@cardiff.ac.uk

Affiliations

Aditee Mitra, School of Earth and Environmental Sciences, Cardiff University, Cardiff, CF10 3AT, United Kingdom.

Kevin J Flynn, Plymouth Marine Laboratory, Plymouth, PL1 3DH, United Kingdom

Maira Maselli, Marine Biological Section, University of Copenhagen, DK-3000, Helsingør, Denmark

Per Juel Hansen, Marine Biological Section, University of Copenhagen, DK-3000, Helsingør, Denmark

Nathalie Gypens, Écologie des Systèmes Aquatiques, Université Libre de Bruxelles, Belgium

Jon Lapeyra Martin, Écologie des Systèmes Aquatiques, Université Libre de Bruxelles, Belgium

Filomena Romano, Institute of Oceanography, Hellenic Centre for Marine Research, PO Box 2214, 71003 Heraklion, Greece

Paraskevi Pitta, Institute of Oceanography, Hellenic Centre for Marine Research, PO Box 2214, 71003 Heraklion, Greece

Table of Contents

1	Executive Summary.....	6
2	Introduction.....	7
2.1	Protist Plankton functional groups and Non-Constitutive Mixoplankton.....	7
2.2	Seasonal distribution of mixoplankton.....	8
3	Arctic waters: the contribution of mixoplankton to the plankton community in the fjords around Disko Bay, Greenland.....	10
3.1	Study site.....	10
3.2	Materials and Methods.....	10
3.2.1	Sampling.....	10
3.2.2	Protist community analyses.....	11
3.2.3	Chlorophyll a analysis.....	11
3.2.4	Dissolved inorganic nutrients analyses.....	11
3.3	Results.....	11
3.3.1	Description of the water column along each transect.....	11
3.3.2	Description of the protist community and Chlorophyll a concentration along each transect.....	14
3.4	Discussion.....	19
4	Temperate waters: NCM succession and spatial variability in The North Sea revealed by DNA metabarcoding.....	22
4.1	Study site.....	22
4.2	Materials and methods.....	23
4.3	Results.....	25
4.3.1	Seasonality in the BCZ.....	25
4.3.2	NNS Summer 2018.....	29
4.3.3	Southern North Sea, May 2019.....	30
4.4	Discussion.....	31
5	Mediterranean oligotrophic waters: Subtropical waters.....	32
5.1	Sampling.....	32
5.2	Materials and Methods.....	33
5.2.1	Ciliate abundance enumeration and biomass.....	33
5.2.2	Statistical analysis.....	33
5.3	Results.....	34
5.3.1	Temporal and vertical distribution.....	34

5.3.2	Size classes	35
5.3.3	Genera of Mixoplanktonic Ciliates	37
5.3.4	Alpha diversity	38
5.4	Discussion	42
6	Conclusions	43
7	References	45

1 Executive Summary

- This report considers the geographic and taxonomic spread of non-constitutive mixoplankton (NCM). NCM are mixoplankton (protists that are both phototrophic and phagotrophic) by virtue of acquired phototrophy; they acquire their potential for photosynthesis from their prey.
- NCM are quantitatively important members of the protistan communities in Arctic, temperate and Subtropical waters. Generally, ciliates were the quantitatively dominant NCM across climate zones, with NCM dinoflagellates and amoebic were of less importance.
- In temperate and polar surface waters, Specialized NCM often bloom in spring, reaching levels nearly 20 times greater in terms of biomass than recorded at more southern latitudes; generally, generalist NCM bloom 1-3 months later than SNCM, but maintain significant biomass well into the summer months, when SNCM populations (the ciliate, *M. rubrum*) crash as nutrient concentrations become depleted in the euphotic zone.
- In the Arctic (e.g., Disko Bay, Greenland) oligotrich and protomatid ciliates dominate the NCM in surface waters during summer, which is characterized strong stratification, 24 h of light, and inorganic nutrient limitation; here they are an important link to higher trophic levels.
- In the North Sea, oligotrich ciliates are major NCM contributors followed by few dinoflagellate species. However, NCM are minor contributors to the number of DNA-metabarcoding reads of protists throughout all year long in the North Sea.
- In oligotrophic Mediterranean waters, heterotrophic ciliate abundance and biomass did not show any seasonality but were closely linked to chl_a concentration. In contrast, NCM ciliates were largely restricted to the months with high temperatures and irradiance. Thus, in the near-surface samples NCM ciliates formed an important part of total ciliate abundance and biomass, and likely moved to deeper layers during June and July.

2 Introduction

Aditee Mitra & Kevin J Flynn

2.1 Protist Plankton functional groups and Non-Constitutive Mixoplankton

The existence of mixoplanktonic protists, combining phototrophy and phagotrophy in a single cell, in marine waters has been well known for decades (e.g., Stoecker *et al.*, 2009; Flynn *et al.* 2013). Mitra *et al.* (2014, 2016) highlighted the importance of mixoplankton in marine biogeochemical cycling and proposed a protist functional group classification identifying different types of mixoplankton according to their functionality. Broadly, mixoplanktonic protists have been classified into those which have innate capability to photosynthesize - Constitutive Mixoplankton (CM; e.g., *Karlodinium*, *Prymnesium*, *Tripos*), and, those that acquire their phototrophic capability from their prey - Non-Constitutive Mixoplankton (NCM; e.g., *Mesodinium*, *Dinophysis*, *Strombidium*). Various biogeography studies have highlighted the importance of the occurrence of different mixoplankton functional types globally (Leles *et al.*, 2017, 2019; Faure *et al.*, 2019). These works have revealed the ubiquity of all mixoplankton functional groups across the different Longhurst provinces from coastal areas to the open ocean with important seasonal differences.

Within MixITiN, the functional classification of Mitra *et al.* (2016) was updated to take into account the mixotrophic and mixoplanktonic protists. The revised protist plankton functional classification including the different mixoplankton functional type (MFT) names (with examples for harmful algal bloom species) is given in **Figure 2.1**.

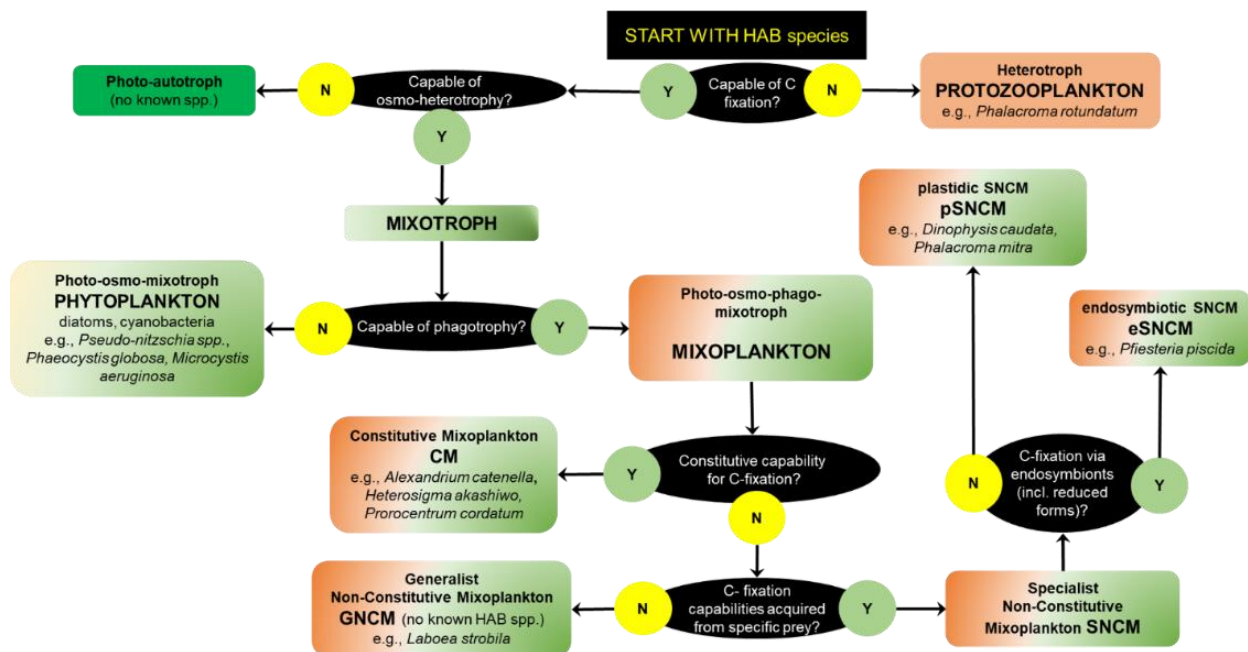


Figure 2.1 Functional group classification key for Harmful Algal Bloom (HAB) species developed from the protist functional group key in Mitra *et al.* (2016) with example species from the IOC-UNESCO HABs list aligned to functional groups according to the Mixoplankton Database (Mitra *et al.* in prep). Reproduced from Mitra & Flynn (2021).

2.2 Seasonal distribution of mixoplankton

The ability of mixoplankton to both photosynthesize and phagocytose allow these organisms to potentially compensate for lack of light and inorganic nutrients especially in environments and seasons when the conditions are not optimal for photosynthetic growth.

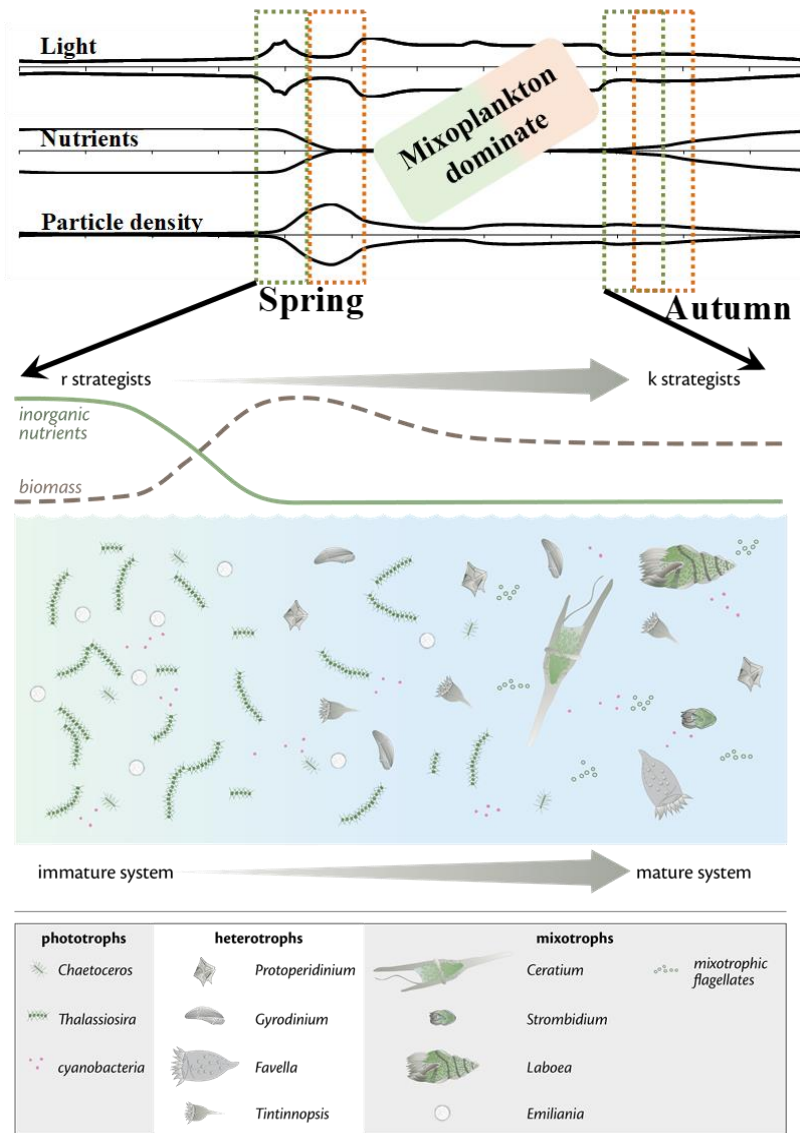


Figure 2.2 Diagrammatic portrayal of the changes to the planktonic food web over a year, with transitions between ecosystem states. The upper panels show changing patterns of light, inorganic nutrients and particle density (i.e., total plankton biomass) over the temperate year. Transitions between developmental and mature stages of the ecosystem are as indicated; **green** and **orange** dashed lines indicate the developmental stages, where green represents conditions optimal for phototrophy and orange for phagotrophy.

Later periods (transition to the more mature state) are suboptimal for phytoplankton and/or protozooplankton, and more supportive for mixoplankton. The lower panel shows in detail the transition from developmental to mature stages, with changes in selection prioritising from “r-selected” FTs in the developmental phase of the ecosystem to a mature ecosystem with “K-selected” FTs. Figure adapted from Mitra et al. (2014).

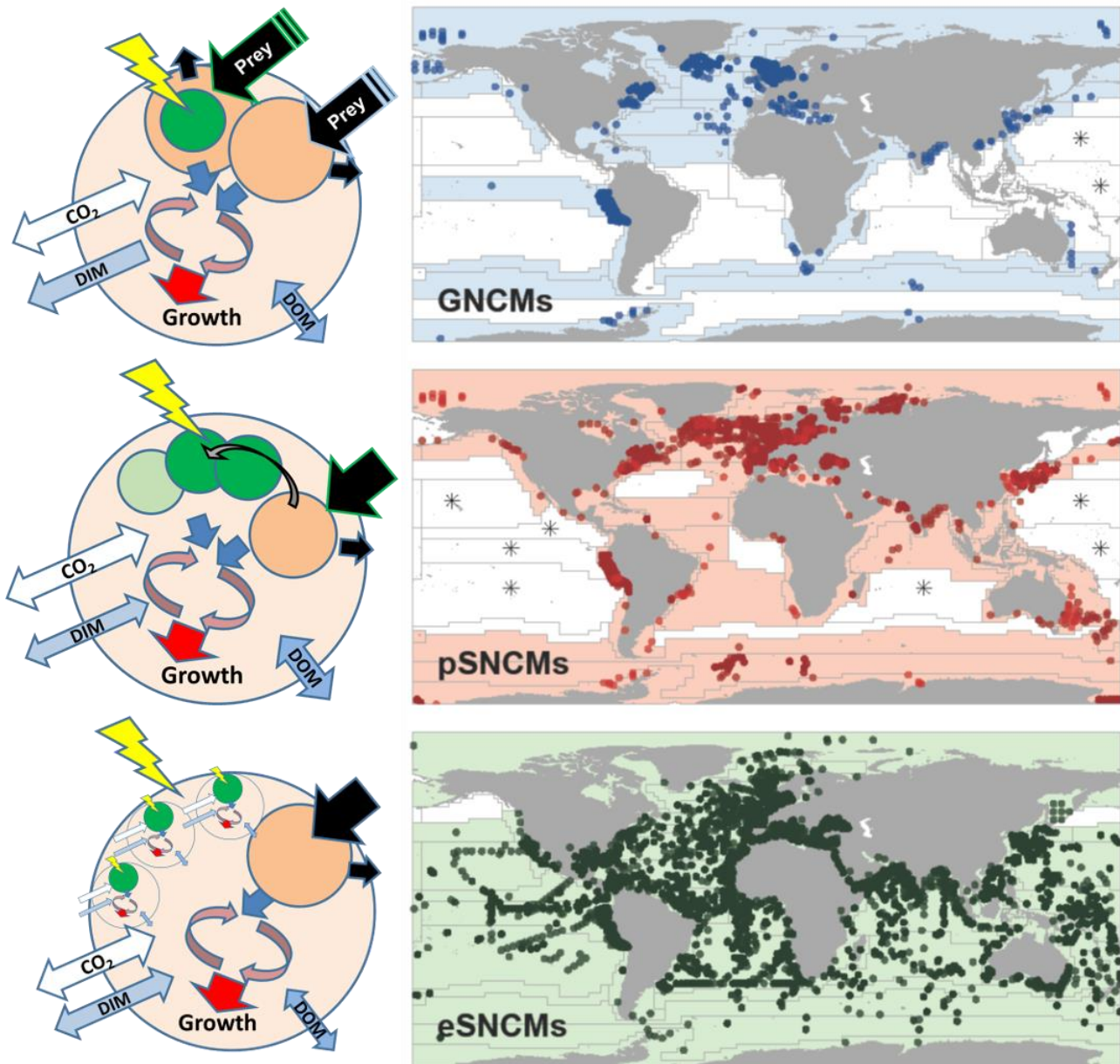


Figure 2.3 Global distribution of different functional types of NCM. On the left are shown schematics of the physiological functioning of these organisms. The generalist NCM (i.e., GNCM) may acquire phototrophy from many types of phototrophic prey; pSNCM are plastidic specialists acquiring phototrophy from specific prey only. eSNCM are endosymbiotic NCM, acquiring phototrophy by harbouring specific phototrophic prey. See Mitra *et al.* (2016) and Flynn *et al.* (2019) for further information. *, no recorded presence. Modified from Leles *et al.* 2017 and Flynn *et al.* 2019.

This report focuses on the seasonality of NCM in Arctic, temperate and tropical/subtropical waters. NCM functional group include protists from various taxonomic groups such as ciliates, dinoflagellates, rhizarians (e.g., Stoecker *et al.* 1987, 1989, 2009; Leles *et al.* 2017; Hansen and Tillmann, 2020). **Figure 2.3** indicates the contrasting physiologies of these organisms and their recorded global distributions.

3 Arctic waters: the contribution of mixoplankton to the plankton community in the fjords around Disko Bay, Greenland

Maira Maselli & Per Juel Hansen

3.1 Study site

The study was conducted in July 2019 in Disko Bay, on the West Greenland coast, in four fjords impacted by runoff of land-terminating glaciers (**Figure 3.1**). In this area, the well-developed sediment plumes allowed to follow gradients in the total load of suspended particles. The sites show different geology, resulting in different chemical imprint on downstream waters.

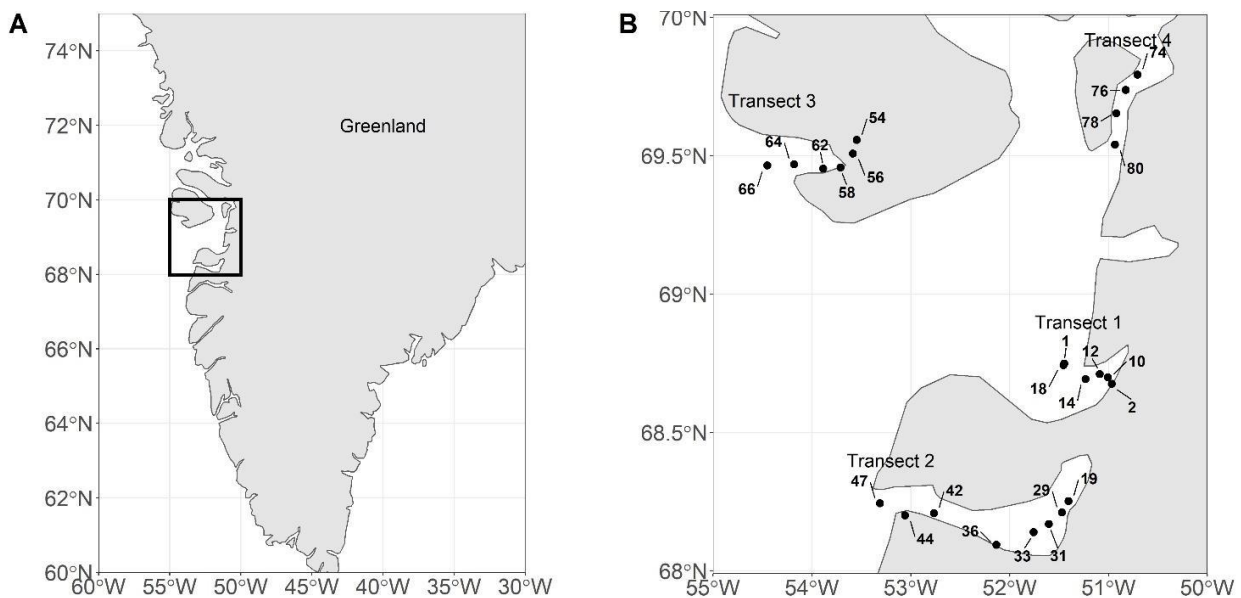


Figure 3.1 Map showing (A) the location of Disko Bay, and, (B) the position of transects and sampling stations exploited during 20-29 July 2019

3.2 Materials and Methods

3.2.1 Sampling

Samples were collected along transects from the inner part of the fjord to the mouth (**Figure 3.1**). At each sampling station, profiles of temperature, salinity, fluorescence and turbidity were collected using a SBE19plus CTD. Water was collected from sub-surface (1 m depth) and at the deep chlorophyll maximum (DCM; variable depth) using 5 and 10 L Niskin bottles and siphoned off with a silicon tube to decrease loss of organisms due to mechanical disturbance. For identification and count of organisms, two samples of 200 mL were collected from each depth in 250 mL amber glass bottles and fixated with two different fixatives: a Lugol's solution (1% final concentration) and a glutaraldehyde solution (2% final concentration). For chlorophyll analysis, 1 L of water was collected and split into two equal subsamples of 500 mL from which chlorophyll contents of two different size classes were

obtained as described below (**Section 3.1.4**, chlorophyll a analysis). Water samples were also collected for dissolved macronutrients (nitrate, phosphate, and silicate) analysis; samples of 10 mL were kept frozen at -20 °C for further analysis.

3.2.2 Protist community analyses

Planktonic protists with a cell diameter of >15 µm were enumerated in the transects' samples using sedimentation chambers (Hydrobios) in accordance with Utermöhl (1958). Cells were counted on an inverted light microscope Olympus (BX 40) equipped with the camera Olympus DP73 at 200x magnification.

The linear dimension (length and width) of the planktonic protists in the transect samples and on the onboard incubation experiments were measured using CellSense software (Olympus Camera software). Cellular biovolumes were calculated using geometric formulae for spheres, cylinders, prolate spheroids or cones according to Hillebrand *et al.* (1999) and converted into cellular carbon content according to Menden-Deuer and Lessard (2000); this allowed calculations of the biomass (µg C L⁻¹) of the individual protist functional groups.

Protists were assigned to functional categories (protozooplankton, mixoplankton and phytoplankton; **Figure 2.1**) following analysis of the glutaraldehyde preserved samples. Glutaraldehyde preserved organisms were collected on polycarbonate filters (pore size 2µm). Filters were stained with Calcofluor (Andersen and Kristensen, 1995) and DAPI (Porter and Feig, 1980), and inspected with an epifluorescence microscopy (Olympus BX 50) equipped with UV, Green and Blue excitation filters prior and after the count of the Lugol sample. This filter set allowed the detection of DAPI, Calcofluor, chlorophyll and phycoerythrin pigments, thus a deeper characterization of the organism morphotypes observed in the Lugol samples. All samples were enumerated by the same person to eliminate observer bias. Triplicate samples from the incubation experiment were averaged for each time point.

3.2.3 Chlorophyll a analysis

The total chlorophyll a (total chl_a) content of the waters samples as well as the chl_a content in the size fraction <15 µm (fractionated chl_a) were analyzed. For total chl_a analysis, biomass was directly collected via filtration on Whatmann glass microfiber filters GF/F, while for the fractionated chl_a samples were first sieved through a 15 µm net mesh. Filters were stored at -80°C until further processing. Chl_a samples were extracted in 5 mL 96% ethanol for 24 h in the dark at 4°C and quantified using a Turner Trilogy Fluorometer.

3.2.4 Dissolved inorganic nutrients analyses

Subsamples (10 mL) for nutrients were filtered through 0.45 µm filters (Q-Max GPF syringe filters) and directly frozen at -20°C until analysis. Nutrients were measured using standard colorimetric methods on a Seal QuAAtro autoanalyzer.

3.3 Results

3.3.1 Description of the water column along each transect

At the time of sampling (20 to 29 July 2019), the four fjords were characterized by different physical and chemical conditions (**Figure 3.1**; **Table 3.1**).

Table 3.1 DCM depth (m) and surface and DCM temperature (Temp; °C), salinity, turbidity (arbitrary units) and concentrations of nitrate, phosphate and silicate (μM) at each station.

transect	station	SURFACE						DCM						
		Temp	Salinity	Turbidity	DIN	DIP	SiO ₂	depth	Temp	salinity	Turbidity	DIN	DIP	SiO ₂
1	10	11	32	2	0.50	0.07	0.93	20	6	34	0.84	0.32	0.06	3.70
1	12	12	30	1	0.30	0.06	1.14	45	3	34	0.24	1.88	0.20	3.90
1	14	12	32	0	0.30	0.06	1.53	50	3	34	0.27	1.22	0.27	3.90
1	18	10	32	0	0.40	0.08	1.82	50	3	34	0.45	2.08	0.35	0.70
2	19	3	12	534	3.60	0.21	15.7	5	3	17	737	4.00	0.26	17.3
2	29	6	10	10	3.30	0.14	7.20	20	3	27	333	6.53	0.44	12.2
2	31	4	14	10	2.70	0.13	12.6	5	4	18	29	4.79	0.28	12.0
2	36	7	18	3	5.40	0.07	3.74	10	5	23	4	1.22	0.19	5.40
2	42	5	25	3	7.20	0.18	3.05	10	4	26	2	4.80	0.50	4.60
2	44	4	26	3	3.00	0.21	3.64	5	4	29	2	3.90	0.22	2.40
2	47	4	29	2	4.30	0.31	1.88	5	4	29	2	4.02	0.27	3.00
3	54	11	6	18	1.90	0.40	11.6	5	5	32	3	1.39	0.15	42.5
3	56	11	12	7	0.40	0.28	17.5	5	6	32	2	1.80	0.2	24.5
3	58	11	11	13	1.00	0.31	8.08	5	6	31	6	6.35	0.18	39.7
3	62	10	26	3	2.60	0.15	2.02	30	3	33	1	3.53	0.45	11.1
3	64	8	31	1	1.20	0.14	0.85	30	3	33	1	1.85	0.28	11.8
3	66	7	33	0	6.00	0.11	0.37	20	3	33	1	1.03	0.16	0.70
4	74	1	28	4	11.4	0.76	11.9	5	1	30	3	11.1	0.79	12.3
4	76	4	28	5	10.1	0.67	5.35	5	1	30	3	5.26	0.42	11.7
4	78	1	29	3	3.70	0.25	5.61	5	1	29	3	6.78	0.4	3.60
4	80	2	29	3	5.80	0.30	7.39	5	1	30	4	3.85	0.35	5.10
4	82	3	30	2	1.10	0.12	3.00	5	3	30	2	0.37	0.12	3.00

Transect 1 (**Figure 3.1B**) was generally warmer than the others and had a warm surface layer in the upper 10-15 m with temperatures of up to 11 °C, which was 5 °C higher than temperatures at 20 m depth (**Figure 3.2**). Salinity was slightly lower at the surface compared to that below 5 m depth in all transects (**Figure 3.3**). Turbidity was low at all stations (**Table 3.1**; **Figure 3.4**). Dissolved inorganic nutrients concentration was also quite low (below 2 and below 0.3 μM of nitrogen and phosphorus respectively) and quite homogeneous along the transect, both at surface and at DCM (**Table 3.1**).

Transect 2 (**Figure 3.1B**) showed a strong salinity gradient (**Figures 3.2** and **3.3**). Salinity increased with depth and along the transect into Disko Bay, varying from about 10 at surface in the innermost station to about 30 at the outermost stations at all depths. The three innermost stations were also very turbid due to large amounts of glacier flour from the melting glaciers. Turbidity decreased with depths and along the transect (**Table 3.1**; **Figure 3.4**). Silicate concentration decreased from inner part of the fjord to the mouth, while dissolved inorganic nitrogen and phosphorous concentrations did not show a clear trend along the transect, varying from about 2 to 7 μM and from about 0.1 to 0.5 μM respectively (**Table 3.1**).

Transect 3 (**Figure 3.1B**) showed both a temperature and salinity gradient along the transect in the upper 5 m of the water column (**Figures 3.2** and **3.3**). Salinity varied from about 10 to 30 and temperature varied from 11 to 6 °C. Below 5 m depth, salinity and temperature were quite homogenous at depth and along the transect being respectively 31 and ~5 °C. The five upper meters were also the more turbid at the innermost stations (**Table 3.1**; **Figure 3.4**). Silicate concentration in the surface water of the innermost stations was much higher than in the other transects. Dissolved inorganic phosphate and silicate concentrations decreased along the transect in surface water, while phosphate and nitrate concentrations at the DCM were only different (higher) in the mid part of the fjord. Dissolved inorganic phosphate and nitrate concentrations were in the same range as in transect 2.

Transect 4 (**Figure 3.1B**) was characterized by cold and homogeneous temperatures (around 1 °C) and limited variation in salinity (**Table 3.1**; **Figure 3.3**). Turbidity was generally quite low (**Table 3.1**; **Figure 3.4**). The concentration of dissolved inorganic nutrients decreased along the transect into Disko Bay and was very similar at surface compared with the DCM (**Table 3.1**). In the innermost stations dissolved inorganic phosphate and nitrate concentrations were double compared with the outermost stations and compared with the highest concentrations found in transects 2 and 3.

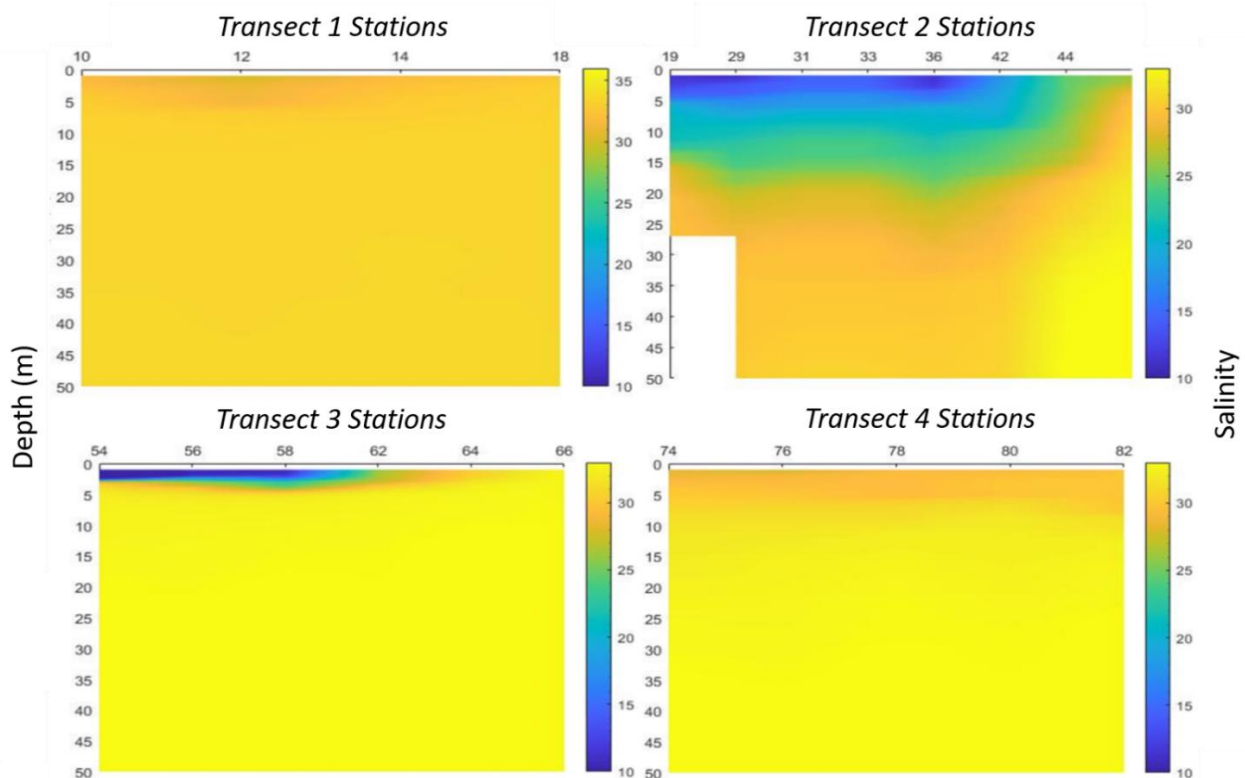


Figure 3.3 Vertical profile of salinity along the 4 fjord transects.

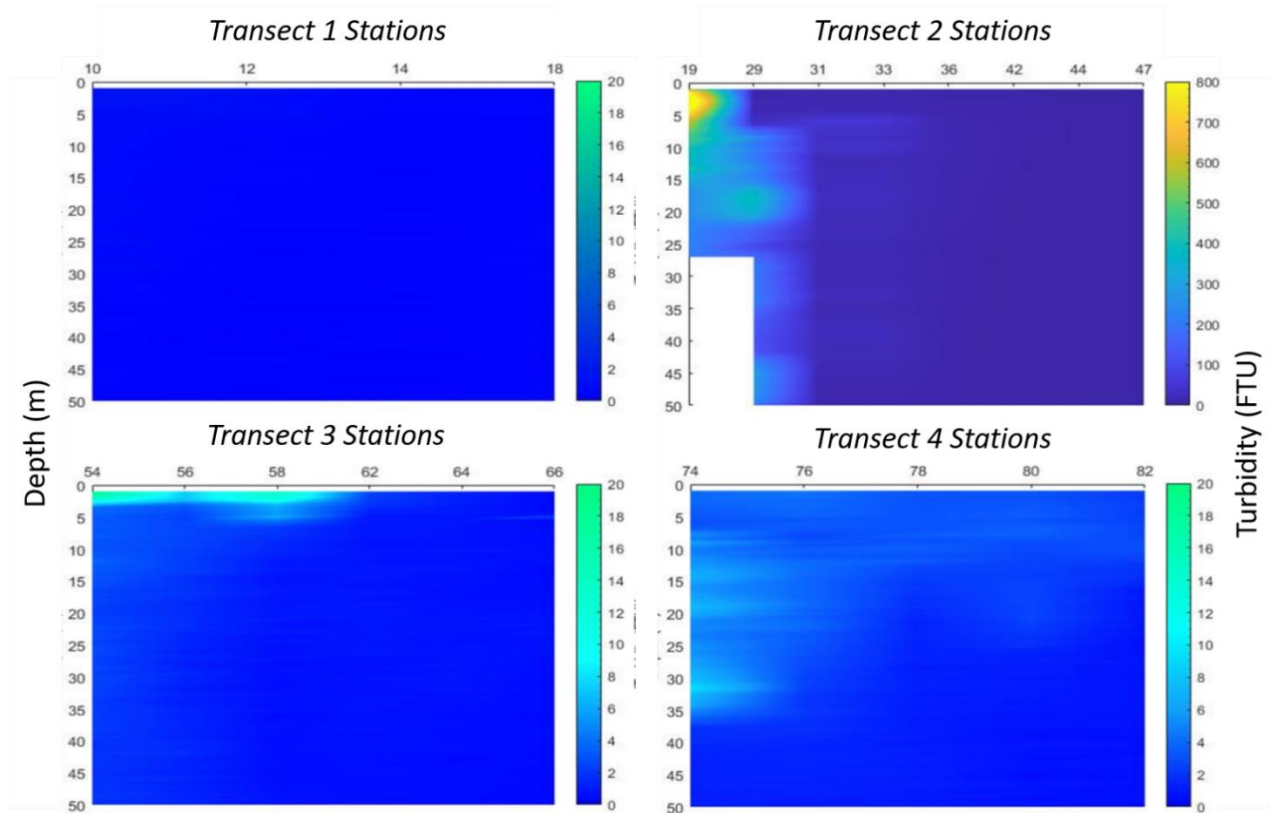


Figure 3.4 Vertical profile of turbidity (Formazin Turbidity Unit, FTU, uncalibrated) along the 4 fjord transects.

3.3.2 Description of the protist community and Chlorophyll *a* concentration along each transect

The biomass of organisms $> 15 \mu\text{m}$ (as $\mu\text{gC L}^{-1}$) and the total chl *a* content ($\mu\text{g L}^{-1}$) were generally higher at the outermost stations at the 4 transects, where mainly autotrophs dominated. Biomass content and composition strongly differed among transects (**Figure 3.6**).

Transect 1 had the lower (total) biomass (**Figure 3.6**), despite that total chl*a* ($\mu\text{g L}^{-1}$) was comparable to transects 2 and 3 (**Figures 3.5** and **3.7**). The largest fraction of the biomass in the surface water was allocated in the heterotrophic compartment, and almost 80% of the chl*a* was allocated in the $< 15\mu\text{m}$ size fraction (**Figure 3.6**). Transect 1 was also characterized by a very deep chlorophyll maximum at the outer stations (50 m), so that the community composition strongly differed from surface to DCM, being dominated by heterotrophs at the surface and by diatoms at the DCM (**Figure 3.6**).

The community composition at transect 2 did not greatly vary from surface to the DCM, nor among stations especially in the terminal part of the transect, from station 36 to station 47 (**Figure 3.6**). Biomass was much lower in the innermost stations, where the higher turbidity was recorded. At the intermediate station (station 33) the autotrophic biomass was much higher at the DCM (5 m) than surface water. Chl*a* in the $< 15\mu\text{m}$ size fraction represented a smaller proportion of the total chlorophyll in the terminal stations compared to the innermost stations (**Figure 3.7**). This was due to a dominance of chain forming diatoms.

Mixoplankton dominated Transect 3, especially in the surface water and the shallower DCM of the innermost stations (**Figure 3.6**). At the outermost stations, the DCM was deeper (**Figure 3.5**) and the protist community changed in being dominated by heterotrophs at surface and by autotrophs at the DCM (**Figure 3.6**).

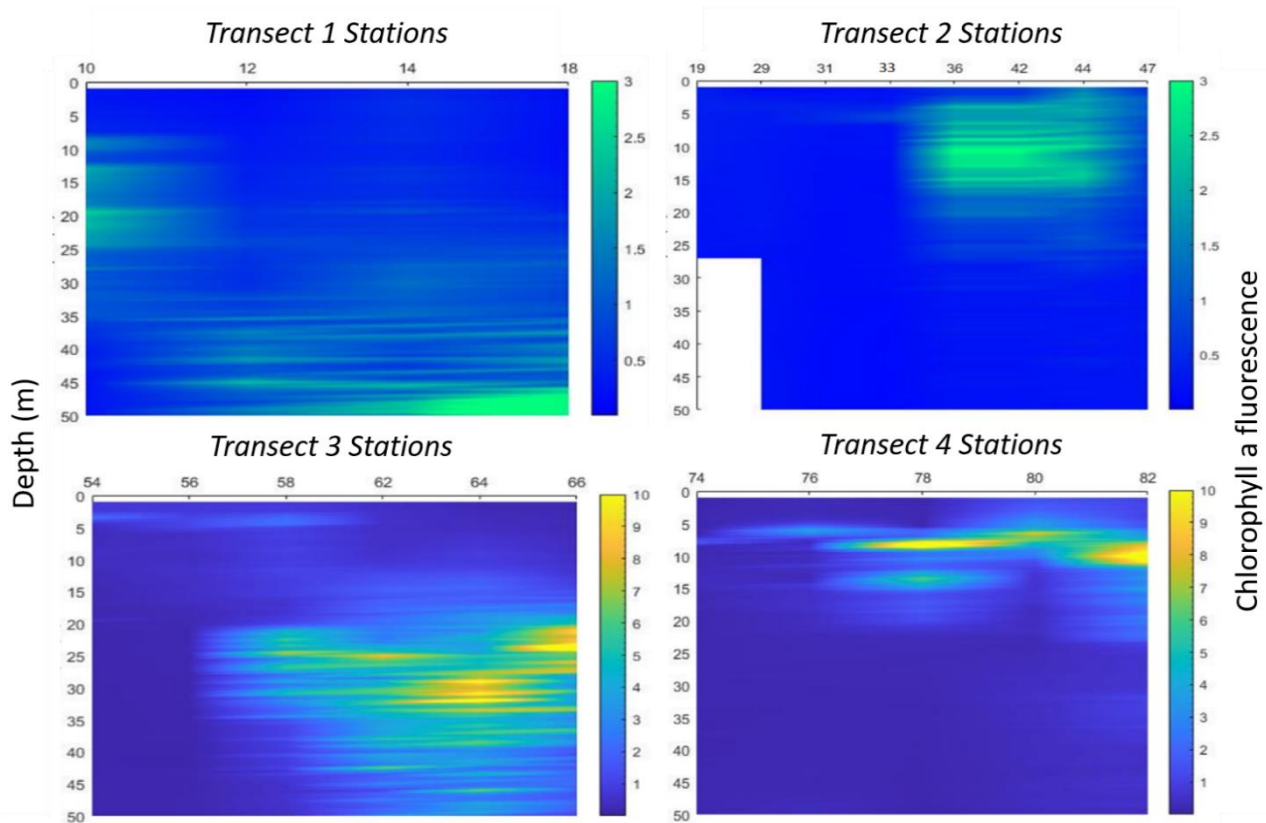


Figure 3.5 Vertical profile of fluorescence (uncalibrated) along the 4 transects.

Transect 4 differed from the other transects in that the biomass was much higher and dominated by chain forming diatoms along the entire transect (**Figure 3.6**); indeed, Chla in the < 15 μm size fraction was almost non-existent (**Figure 3.7**). The biomass of heterotrophic protists (ciliates and dinoflagellates) was comparable to the other transects, while mixoplankton made up a very small fraction (**Figure 3.6**).

Heterotrophic protists, i.e., protozooplankton, were represented by ciliates and dinoflagellates in all samples. Although some radiolarians were found, the rare individual cells did not represent a significant proportion of the total biomass in any of the samples. Heterotrophic dinoflagellates were consistently more abundant than heterotrophic ciliates, which represented less than one third of the total heterotrophic biomass in the majority of the samples (**Table 3.2**). The most abundant and widespread heterotrophic dinoflagellates belonged to the genera, *Gyrodinium* and *Protoperdinium*. Aloricate ciliates (heterotrophic and mixoplanktonic) were generally more abundant than loricate ciliates (tintinnids), and dominated by the genera *Strombidium*, *Strobilidium*, *Monodinium*. Despite numerical abundance in some samples, the biomass of small heterotrophic ciliates (~ 20 μm) did not account for a significant proportion of the total heterotrophic protist biomass in any of the samples (**Table 3.2**).

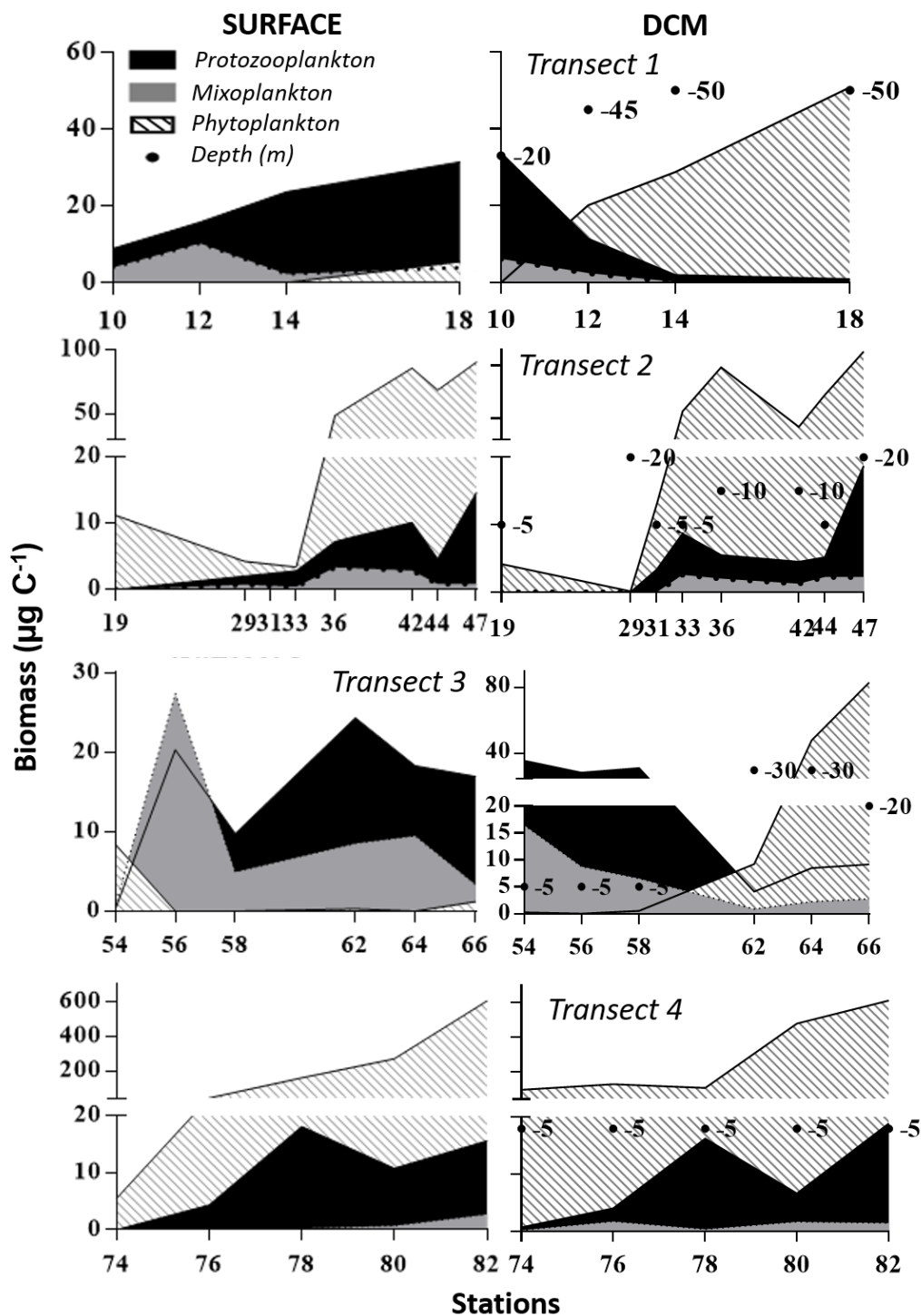


Figure 3.6 Biomass ($\mu\text{g C L}^{-1}$) of heterotrophic protozooplankton (in black), mixoplankton (in grey) and autotrophic phytoplankton (striped) and depth of the DCM (dots) at all stations along each transect. Note the difference in biomass for transect 3.

Total mixoplankton were generally less abundant than heterotrophs (~25% of the biomass of heterotrophs on average) and mostly represented by mixoplanktonic ciliates. Mixoplanktonic dinoflagellates only exceeded mixoplanktonic ciliates biomass in:

- surface samples of transect 3 - where dinoflagellates in the genera *Alexandrium* and *Heterocapsa* were abundant, and,

b) two stations in transect 1 (10 DCM and 12 surface), where *Dinophysis* and *Heterocapsa* contributed to the relatively high biomass of mixoplanktonic dinoflagellates. Mixoplanktonic ciliates belonging to the genera *Laboea*, *Strombidium* and *Mesodinium* almost equally contributed to the biomass of mixoplanktonic ciliates in all samples. However, *Mesodinium rubrum/major* accounted for most the mixoplanktonic ciliate biomass on a few occasions (**Table 3.2**).

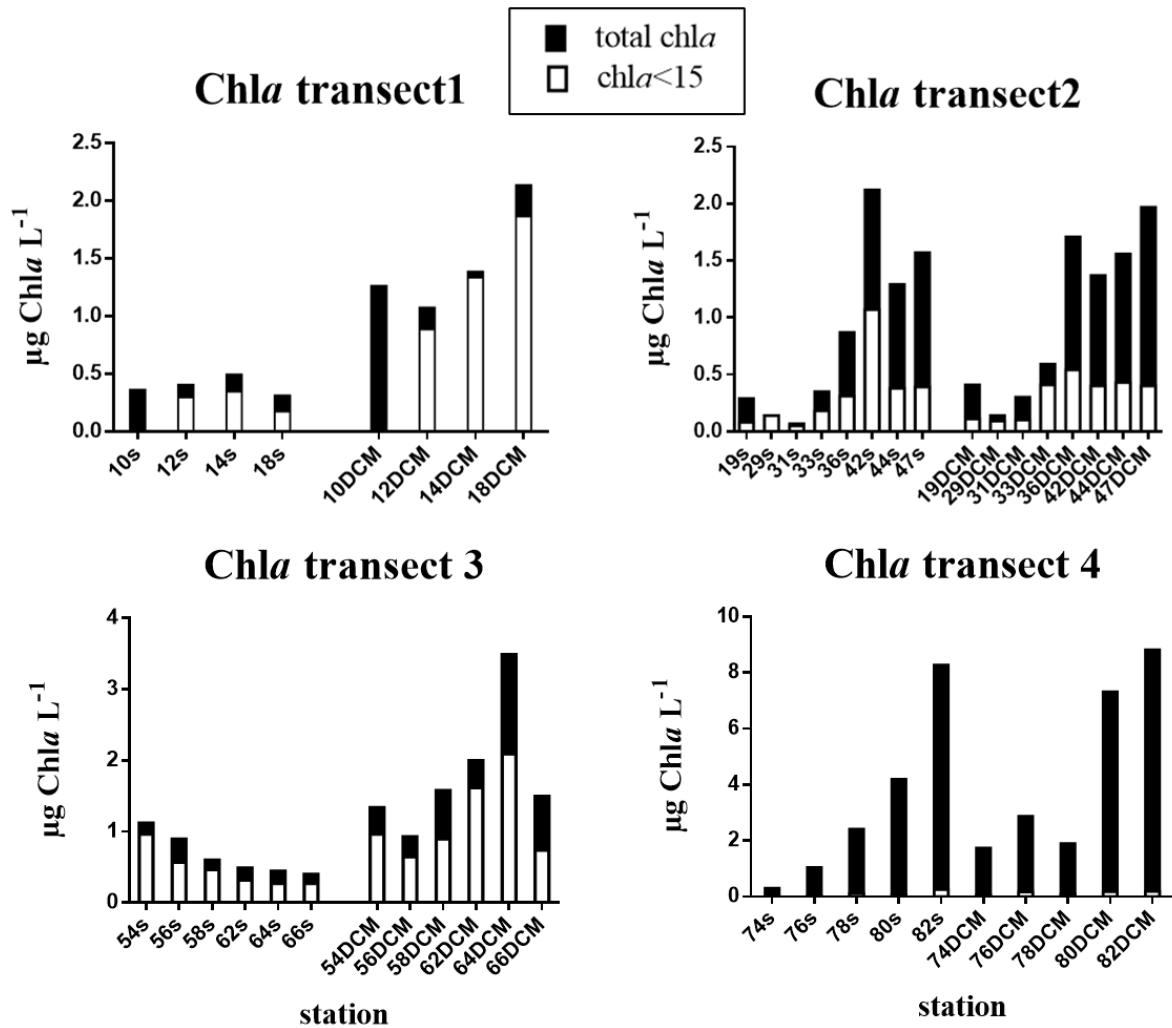


Figure 3.7 Total Chlorophyll a concentration and fraction of Chla concentration in the size category $<15\mu\text{m}$ in all stations at surface and DCM

Table 3.2 Biomass ($\mu\text{gC L}^{-1}$) of the most dominant protists groups (dinoflagellates, ciliates and diatoms) at selected stations at (a) surface and (b) DCM. Protists were grouped according to their trophic mode (i.e., functional group); see also **Figure 2.1**. *Gyro* = *Gyrodinium* spp; *Proto* = *Protoperdinium* spp; *Tint* = tintinnids; *Small* = $\sim 20 \mu\text{m}$; *Hetero* = *Heterocapsa* spp; *Dino* = *Dinophysis* spp; *Meso* = *Mesodinium* spp

(a) SURFACE SAMPLES

Stations	phago-osmo-hetero-trophs (Protozooplankton)						photo-auto-phago-osmo-hetero- trophs (Mixoplankton)					photo-auto-osmo-hetero- trophs (Phytoplankton)
	Dinoflagellates			Ciliates			Dinoflagellates			Ciliates		Diatoms
	Total	<i>Gyro</i>	<i>Proto</i>	Total	<i>Tint</i>	<i>Small</i>	Total	<i>Hetero</i>	<i>Dino</i>	Total	<i>Meso</i>	Total
1-12	11.0	6.5	2.8	4.8	1.3	0.1	8.2	6.4	0.3	2.2	1.2	0.0
1-14	16.3	6.2	1.2	7.4	2.4	1.1	2.1	0.6	1.1	3.2	0.3	0.1
1-18	23.9	9.4	3.1	7.6	1.1	0.3	3.2	0.2	2.0	1.9	0.1	5.5
2-19	0.0	-	-	0.0	-	-	0.0	-	-	0.0	-	11.2
2-33	2.6	-	-	0.2	-	-	0.0	-	-	0.4	0.4	3.5
2-42	9.9	5.6	3.4	0.3	-	0.2	0.7	0.6	0.1	2.2	0.2	86.1
2-47	14.4	10.7	1.0	0.3	0.1	-	0.3	-	-	0.5	-	90.7
3-56	19.8	1.1	0.1	0.5	-	0.5	24.9	8.6	-	2.5	-	0.0
3-62	19.3	10.4	1.0	5.0	1.0	-	6.7	2.5	0.1	1.9	0.9	0.3
3-66	13.3	6.0	1.1	3.7	0.4	-	1.4	1.2	0.3	1.9	-	1.2
4-74	0.0	-	-	0.0	-	-	0.0	-	-	0.0	-	5.5
4-82	14.1	-	-	1.5	-	-	1.5	-	-	1.2	-	606

(b) DCM SAMPLES

Stations	phago-osmo-hetero-trophs (Protozooplankton)						photo-auto-phago-osmo-hetero - trophs (Mixoplankton)					photo-auto-osmo-hetero- trophs (Phytoplankton)
	Dinoflagellates			Ciliates			Dinoflagellates			Ciliates		Diatoms
	Total	<i>Gyro</i>	<i>Proto</i>	Total	<i>Tint</i>	<i>Small</i>	Total	<i>Hetero</i>	<i>Dino</i>	Total	<i>Meso</i>	Total
1-12	8.9	2.3	0.6	2.5	0.2	0.1	0.7	0.3	0.4	1.8	0.1	4.6
1-14	0.6	0.3	0.2	1.4	0.2	-	0.2	-	-	0.0	-	31.0
1-18	0.2	-	-	0.7	-	-	0.0	-	-	0.0	-	0.7
2-19	0.0	-	-	0.0	-	-	0.0	-	-	0.0	-	4.2
2-33	7.6	-	4.6	1.1	0.3	-	0.4	-	0.3	2.2	2.2	56.8
2-42	3.2	1.4	0.9	1.3	1.0	0.2	0.1	-	0.1	1.2	0.3	41.9
2-47	17.6	15.2	1.3	1.1	0.6	0.1	0.2	0.2	-	2.1	0.7	113
3-56	23.4	2.4	0.7	5.2	3.9	0.1	4.8	0.4	0.5	3.9	1.4	0.0
3-62	2.9	0.6	0.9	5.6	0.1	0.1	0.4	0.2	-	1.8	1.4	6.7
3-66	37.2	14.7	8.1	6.8	1.0	-	2.4	1.9	0.5	3.7	0.8	42.8
4-74	0.7	-	-	0.0	-	-	0.0	-	-	0.2	-	95.7
4-82	17.7	15.9	0.2	1.2	0.5	-	0.2	-	0.2	1.3	0.1	631

3.4 Discussion

Gradients associated with the glacier inputs were distinguishable in the chemical and physical qualities of the water column in all four different fjords. The sediment plume was only evident at stations that were close to the glacier input. A large fraction of glacial sediments settle within a few kilometres from the input, in accordance with previous observations in the area (Meire *et al.*, 2017). The relatively low protist biomass in the innermost station can only partially be attributed to turbidity caused by suspended particles. Suspended particles tend to agglutinate to protists and bacteria, thereby transporting them out fast from the photic layer (Szeligowska *et al.*, 2021).

The freshening of the upper part of the water column lead to a stronger stratification of water column and this decreases the vertical mixing and create a nutrient-poor surface layer. This limits the growth of autotrophic organisms and lead to the deepening of the chlorophyll maxima (Holding *et al.*, 2019; Hopwood *et al.*, 2020). This was less evident on transect 4 due to the presence of marine-terminating glaciers that could have led to the upwelling of nutrient rich bottom water (Meire *et al.*, 2017). Diatoms dominated the protist communities on transect 4 and in most of the offshore stations on the other transects.

The protozooplankton and mixoplankton were more abundant at the innermost stations of transects 1-3. Their relative abundance in terms of biomass, exceeded that of the phytoplankton in stations where the dissolved inorganic nitrogen concentrations were relatively low ($< 2 \mu\text{M}$). On such stations chl a was mainly found in the $< 15 \mu\text{m}$ fraction, suggesting that phototrophic nanoplankton, which have a higher surface to volume ratio compared to phototrophic microplankton, were favoured in nutrient limiting conditions (Stolte and Riegman, 1995). Moreover, many photosynthetic nanoplankton species ($< 20 \mu\text{m}$ in size) other than diatoms, are known to be mixoplanktonic and sustain their metabolism through bacterivory (Stoecker *et al.*, 2017). A similar predominance of chl a in the small size fraction have previously been observed in the inner location of other Western Greenlandic fjords (Arendt *et al.*, 2010, 2016). The predominant grazing activity on primary producers in such locations is likely attributed to the microplanktonic grazers rather than copepods, which instead play an important role in the coastal zones (Arendt *et al.*, 2010, 2016). Similarly, especially at transects 1 and 3, heterotrophic and mixoplanktonic microplankton seemed to be associated with the smaller size fraction of primary producers (the chl a fraction $< 15 \mu\text{m}$).

Heterotrophic dinoflagellates were also found on more offshore stations where most of the chl a was due to chain forming diatoms (functionally $> 15 \mu\text{m}$). Dinoflagellates in the genera *Protoberidinium* and *Gyrodinium* have already been recorded to be dominant in summer in Greenland and associated to diatom blooms (Krawczyk *et al.*, 2015). Heterotrophic ciliate biomass, instead, was very low or even null in such samples. This is likely explained by differences in the feeding mechanisms in these two groups. The ciliates species found in this survey were mostly filter feeders. Thus, their grazing potential was limited to particles, which size fits the morphological constrains of their feeding apparatus (Jonsson, 1986). The feeding mechanisms of dinoflagellates are more diverse. Many thecate species, like *Protoberidinium* and the *Diplosalis* group use a

pallium (a sort of pseudopod) to unveil the prey. Most of the athecate species like *Gyrodinium* spp use direct engulfment, while many athecate and thecate species, like *Phalacroma* and many small heterotrophic species use peduncles (feeding tubes). These are all feeding mechanisms that allow the organisms to ingest prey items exceeding their own size (Jacobson and Anderson, 1986; Hansen and Calado, 1999).

Mixoplanktonic microplankton was relatively more abundant in the mid part of the fjords, especially in areas where the water column was strongly stratified. This is especially evident at transect 3, where stratification was induced by both salinity and temperature. Peaks in the relative abundance of mixoplanktonic microplankton were formed by constitutive mixoplanktonic species (*Heterocapsa* spp. and *Alexandrium* spp.), while non-constitutive mixoplankton never dominated the microplankton communities. The reasons for that can be found in biotic factors such as the top-down control from metazoan grazers and specific interaction among microorganisms. Mixoplankton ciliates in particular, are a preferred prey of copepods (Stoecker and Lavrentyev, 2018), while most constitutive mixoplanktonic dinoflagellates produce toxins (Burkholder *et al.*, 2008) that deters predation.

The only identifiable non-constitutive mixoplanktonic dinoflagellate species were *Dinophysis* spp, which are prey specialist grazers that can only acquire phototrophy by feeding on the non-constitutive mixoplanktonic ciliate *Mesodinium rubrum* (Hansen *et al.*, 2013). Not surprisingly, *Dinophysis* spp were only found in samples where the mixoplanktonic *Mesodinium* spp were also present. Non-constitutive mixoplanktonic ciliates in the *Mesodinium rubrum* species complex are also prey specialist grazers that can only acquire chloroplasts via feeding on cryptophytes within the *Teleaulax/Plagioselmis/-Geminigera* clade (Hansen *et al.*, 2013). Differently from many other mixoplanktonic ciliates, *Mesodinium rubrum* can take up and utilize inorganic nutrients for growth and go through up to 4 cell divisions without prey (Tong *et al.*, 2015; Kim *et al.*, 2017). *Mesodinium* spp only dominated the mixoplanktonic ciliates biomass in few of our samples. Indeed, *Mesodinium* biomass is usually low under non-bloom conditions, which tend to occur in localized patches (Crawford, 1989), as actually evident from the distribution of this ciliate found in these fjords. Except for a few locations, prey generalists mixoplanktonic ciliates were equally or more abundant than *Mesodinium*, as typical in polar waters (Levinsen and Nielsen, 2002; Stoecker *et al.*, 2009; Leles *et al.*, 2017). The total biomass of mixoplanktonic ciliates was in the low range of what it could be in summer in more open waters of the same area, but their relative abundance compared to the total ciliate biomass (from ~ 30% to ~ 70%) was comparable to those previous records (Putt, 1990; Levinsen *et al.*, 2000; Levinsen and Nielsen, 2002) .

The way in which the glacial flour inputs affect microplankton communities depends on the chemical-physical properties of the runoff water and the hydrology of the specific location. As previously suggested, the functional classification of plankton has to be adequate in order to underline different response of organisms to the impact of glacier discharges in the marine ecosystem (Szeligowska *et al.*, 2021). Indirectly, the high suspended-particle load, potentially however, has an impact due to possible aggregation of protists to suspended particles, especially close to the glacier inlet. Diatom abundance seems to be more influenced by the glacier inputs compared to the heterotrophic and

mixoplanktonic microplankton that are not directly affected by turbidity and the nutrients limitation. The freshening of marine coastal waters, associated with increased turbidity, aggregate formation, and de-eutrophication, may lead to a shift from fast growing photoautotrophic microplankton communities to less productive communities dominated by heterotrophic and mixoplanktonic microplankton species.

4 Temperate waters: NCM succession and spatial variability in The North Sea revealed by DNA metabarcoding

Jon Lapeyra Martin & Nathalie Gypens

4.1 Study site

New molecular techniques are widely used for plankton diversity assessment (Medlin and Kooistra, 2010) and have a high potential for very detailed monitoring (Stern *et al.*, 2018), encompassing the entire protistan community including nano- and pico-planktonic components, and therefore NCM. The small ribosomal subunit (SSU) 18S rRNA gene is the most widely used marker for the detection and classification within the marine eukaryotic microbes. Despite providing semi-quantitative information (Santoferrara, 2019) the barcoding of different regions of this gene has been proven to be a powerful and sensitive tool for large-scale biodiversity surveys, allowing comparison of studies rooted in taxonomy (Chain *et al.*, 2016).

In this study, we characterized the spatial and temporal variations of the NCM assemblages in the North Sea (NS) based on molecular data (metabarcoding) (**Figure 4.1**). We performed Illumina MiSeq sequencing of V4-18S rRNA in 155 samples from NS collected in 2018-2019, divided into three subsets:

- (i) 1 year time-series in the Belgian Coastal Zone (BCZ),
- (ii) summertime sampling in the Northern North Sea (NNS) and the BCZ, and,
- (iii) late spring post-phytoplankton bloom snapshot in three areas of the Southern North Sea (SNS), i.e., the British waters along the English coastal (EN), the Dutch coastal water (NL), and the BCZ.

Temperate seas such as the North Sea are under the influence of strong nutrient, temperature, irradiance, as well as biotic factors (like grazing, pathogens and competition; Gran-Stadniczeňko *et al.*, 2019). Particularly the SNS is subjected to direct and indirect anthropogenic inputs that are discharged via rivers from the watersheds (Passy *et al.*, 2013). In this region massive *Phaeocystis globosa* blooms occur during spring (Lancelot *et al.*, 2005) and mixed water column and nutrient-enriched waters prevail (Desmit *et al.*, 2015). In the central and NNS, due to slower current velocities (Ducrotoy *et al.*, 2000) and influence of different water masses (Atlantic, Baltic Sea), seasonal or permanent stratification takes place (Sonja van Leeuwen, 2015).

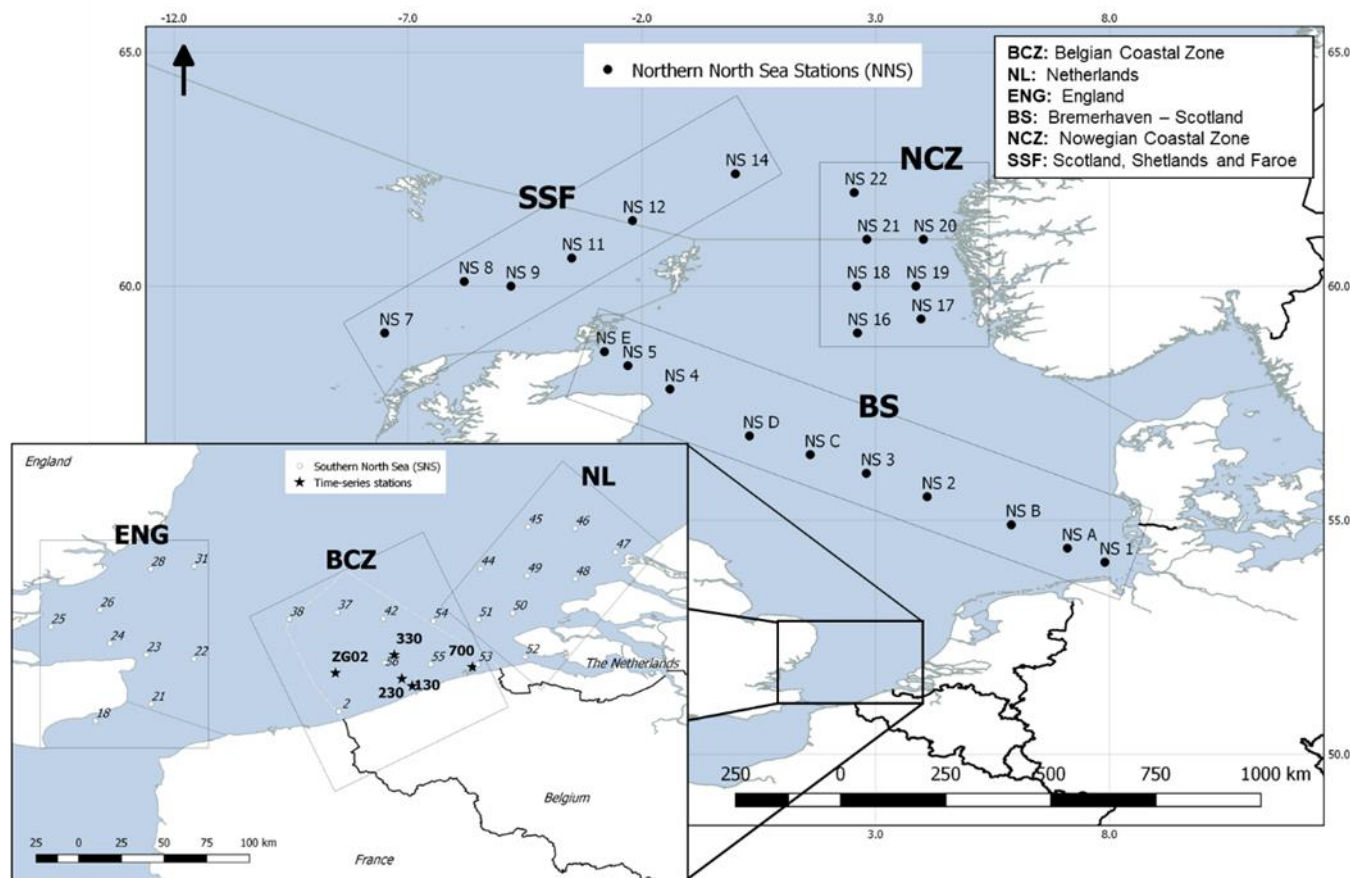


Figure 4.1 Field sampling location (inset) accessed using the RV Simon Stevin in Southern North Sea and RV Heincke in the Northern North Sea.

SNS sites (including ENG, NL and BCZ time-series) were sampled during several expeditions aboard the RV Simon Stevin (Vlaams Instituut voor de Zee, VLIZ; **Figure 4.1**). The time-series monitoring in BCZ took place monthly from March 2018 to June 2019 at five fixed station locations (130, 230, 330, 700 and ZG02), chosen to cover both near-offshore gradient and a longitudinal gradient. One extra monthly cruise was performed over the spring-summer months, with samples collected in order to closely follow the evolution of the phytoplanktonic blooms that occur in this period in Belgian waters. Time-series analysis was performed on the five station averaged values. The sampling expedition covering the ENG, BCZ and NL coastal areas (**Figure 4.1**) took place throughout the first week of May 2019.

4.2 Materials and methods

Seawater samples were collected at 3 m depth using 4 L Niskin bottles connected to a CTD sensor (Sea-bird SBE25). Physico-chemical parameters such as temperature, salinity, major nutrients (DIN, PO_4^{3-}) as well as chlorophyll-*a* (Chl-*a*) were measured and analysed as part of the national water quality monitoring programs LifeWatch and JericoNext with the methodology found in Mortelmans *et al.* (2019).

NNS sampling was carried out on the RV Heincke (Alfred Wegener Institute) during the expedition HE517 in August-September 2018. Three different areas were chosen to be analysed, covering (1) the transect from Bremerhaven (Germany) to the north of Scotland

(BS); (2) the continental rift between Scotland, the Shetlands Islands, and the Faroe Islands (SSF); and (3) the Norway Coastal Zone (NCZ) (**Figure 4.1**). The sampling was realized using Niskin bottles on a rosette sampler attached to a Conductivity-Temperature-Depth (CTD) sensor (SEA-bird SBE 911plus, SN 1015).

Considering that mixoplankton is largely widespread in both nano- and micro-organisms, field sampling techniques in this study were used to sample marine eukaryotic plankton sizing > 0.22 µm. For all above-mentioned expeditions, identical sampling methodology was followed. The DNA samples for the study of the protistan community were collected by vacuum filtering 500-800 mL of water (from Niskin) through 0.22 µm polycarbonate filters (47 mm) and storing the samples immediately at -20 °C.

Total DNA was extracted from filters using NucleoSpin Soil extraction Kit (Macherey-Nagel, Düren, Germany) following manufacturer's protocol. For a maximum efficiency of the extraction from the filters the sample lysis step was performed using 10 mL cryotubes. Standard polymerase chain reactions (PCR) reactions were performed to amplify the universal eucaryote small subunit (SSU) 18S rRNA gene. Primers TAREuk454FWD1 (5'-CCAGCASCYGC GGTAATTCC-3'), TAREukREV3 (5'-ACTTTCGTTCTTGATYRA-3') were used to target the V4 region of the 18S rRNA gene (Stoeck *et al.*, 2010). The following library preparation of 18S ribosomal RNA gene amplicons were executed: PCR clean-up 1, index PCR, PCR clean-up 2, library quantification, normalization and pooling were performed following the 16S Metagenomic Sequencing Library Preparation guide (Illumina). Library denaturing and sample loading to the Illumina MiSeq system to perform a 2 x 250bp paired-end sequencing using V2 chemistry.

For already demultiplexed raw files (MiSeq paired-end output), FASTQC was used to check the quality of reads (Andrews, 2010). TRIMMOMATIC (Bolger *et al.*, 2014) was used to crop the 250 bp to 225 bp and used sliding window of length 3, with allowed average 'phred' score of 8 to filter from 5' - 3' direction and truncate when quality drops below 8. The paired-ends were merged with VSEARCH (Rognes *et al.*, 2016) with a minimum overlap of 40 bp and a maximum number of allowed mismatch of 4 bp. Sequences were reverse complemented and both direction merged into one file. The combined files were then filtered (allowing mismatch of 10% and minimum overlap of 17 bp for forward and 13 bp for reverse) for checking the existence of the primer sequences (fwd-> rev). Primer sequences were removed using CUTADAPT (Martin, 2011). Feature filtering was carried out next with VSEARCH: allowed maximum expected error per sequence of 1; minimum length of 275, maximum 475 and max number of ambiguities of 0. In the same step the headers were renamed by a shall digest of the sequence itself. Each sample was dereplicated independently (abundances of each amplicon added to the header) and chimera checked *de novo*. All samples were pooled and dereplicated in total to produce a combined data set. This served as input for the SWARM OTU clustering (Mahé *et al.*, 2014) using a distance of 1. The most abundant amplicon of an OTU cluster was used as representative. These sequences were annotated with the default bootstrap-based method (RDP) recommended and implemented in MOTHUR (Hardge *et al.*, 2018). Taxonomical annotation was performed MOTHUR's prepared Silva v1.32 (Pruesse *et al.*, 2007) database.

Trophic strategies were annotated based on the current accepted forms of protistan plankton nourishment (Mitra *et al.* 2016; Flynn *et al.*, 2019; see also **Figure 2.1**). Species-specific knowledge were obtained from published literature (Armeli Minicante *et al.*, 2019; Faure *et al.*, 2019; Leles *et al.*, 2019) to classify the species into trophic groups: phytoplankton or strictly autotrophs (AU), protozooplankton or strictly heterotrophs (HET), constitutive-mixoplankton (CM), non-constitutive mixoplankton (NCM) and unknown (NA).

4.3 Results

Overall, 205 OTUs out of 1011 were assigned to mixoplankton: 174 to constitutive mixoplankton (CM) and 31 to non-constitutive mixoplankton (NCM). Regarding the number of reads of the total dataset comprising 155 samples, 33.5% were assigned to CM, 2.1% to NCM, 25.4% to photo-autotrophic phytoplankton and 32.8% to heterotrophic protozooplankton (**Table 4.1**). Dinoflagellates and heterotrophic nanoflagellates were the most abundant groups in terms of number of reads (45.8% and 15.8%, respectively), followed by *Phaeocystis* (12.5%), diatoms (7.9%) and ciliates (7%) (data not shown).

Table 4.1 Summary of the proportions of reads (%) belonging to the different trophic strategies annotated for the entire dataset and the different spatial and temporal scenarios covered the Southern and the Northern North Sea sampling.

FTs	Total dataset	Belgian Coastal Zone (Time-series)				Spatial analyses		
		Spring 18'	Summer 18'	Autumn 18'	Winter 18'-19'	Spring 19'	North Sea Summer 18'	SNS May 19'
phototrophs	25.47	13.82	16.57	20.19	19.92	33.95	16.44	41.23
CM	33.56	53.77	39.77	28.47	25.93	30.16	47.27	15.5
NCM	2.14	1.34	0.69	2.15	4.44	1.92	2.38	1.36
heterotrophs	32.78	25.57	31.28	37.05	40.74	31.89	27.02	39.66
mixoplankton	35.70	55.11	40.46	30.62	30.37	32.08	49.65	16.86
NA	6.05	5.50	11.70	12.14	8.98	2.08	6.86	2.22

4.3.1 Seasonality in the BCZ

The environmental conditions varied widely across the temporal series in BCZ (**Figure 4.2**). In general, the range values recorded in the study period are atypical and they follow the well-known seasonal dynamics of the area (Gypens *et al.*, 2007).

Metabarcoding results revealed the taxonomic composition of mixoplankton in the BCZ time-series, showing that, in average, the taxa having most mixoplanktonic species were dinoflagellates, accounting for 87% of the total mixoplankton reads and 136 identified OTUs (out of total 205 OTUs; data not shown). Dinoflagellates were followed by ciliates with a 5.9% of the reads and 26 OTUs.

Regarding NCM, only 5 dinoflagellates were classed as NCM. NCM had a relatively low contribution to the entire protistan community compared to CM (max = 4.4% winter 2018-2019 averaged; **Figure 4.3**) and they comprised of ciliates, and few dinoflagellate species. < 1% of detected dinoflagellates were classed as NCM (data not shown). Mixoplanktonic ciliates attained in average 27.4%. In ciliates, the neither the

heterotrophic nor the mixoplanktonic showed a clear seasonal pattern (**Figure 4.4**). However, it is worth noting that > 90% of ciliates were found to be heterotrophic in May 2018 (**Figure 4.5**).

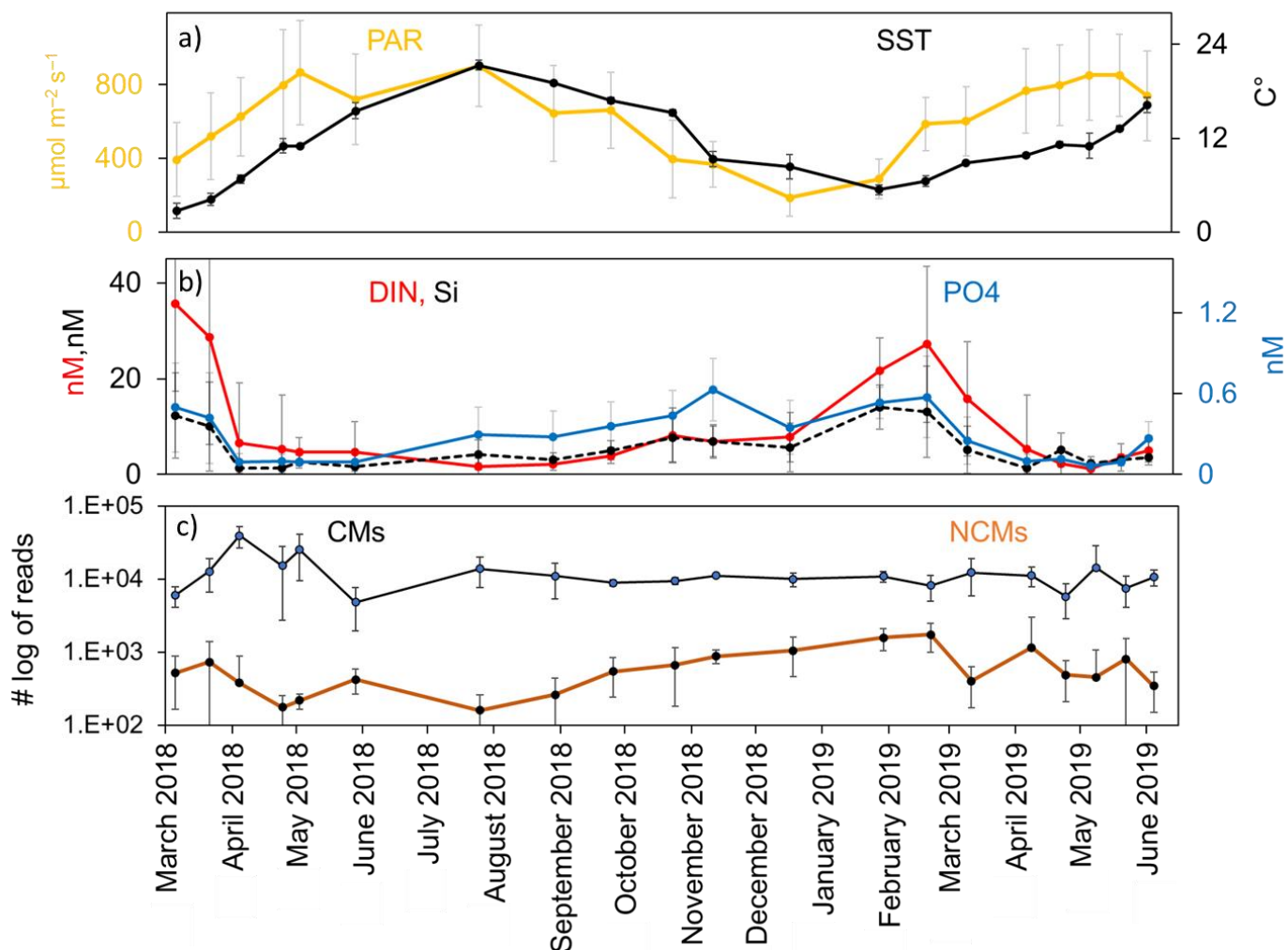


Figure 4.2 Temporal succession of environmental data in the Belgian Coastal Zone (BCZ) time-series and dynamics of strictly photo-autotrophic plankton (phytoplankton), CM and NCM. (a) Photosynthetic active radiation (PAR) and Sea Surface Temperature (SST, $^{\circ}\text{C}$). (b) Dissolved Inorganic Nitrogen (DIN), dissolved silica (DSi), and phosphates (PO_4^{3-} , nM) concentrations. (c) log read abundances for CM and NCM revealed by DNA-barcoding.

Most important constituents based on proportional OTU reads appeared to be marine oligotrich ciliates belonging to the genus *Strombidium*: ranging 1.1 - 3.5% in Winter 2018-2019 and 2.6% in April 2019 (**Figure 4.3**). Another important mixoplanktonic ciliate, *Spirostrombidium cupiformum* attained its maximum value in March 2018 (1.8 - 1.6%) and were important NCM members in Winter 2018-2019 (1.4 - 1.5%) (**Figure 4.5**). Species belonging to the *Lepidodinium* genus such as *Lepidodinium chlorophorum* (a

kleptoplastidic NCM species) were the only dinoflagellates detected among the top 10 most relevant NCM species, having its maximum contribution in autumn 2018 (1.3% in September-October). Only two other NCM dinoflagellates were detected in our dataset, *Dinophysis acuminata* and *Shimiella gracilenta*, both having their maximum contributions < 0.03%. Two *Pseudotontonia* genus organisms (GNCM) were present in our BCZ time-series dataset as well, consistent with both Leles *et al.* (2019) morphological observations and Faure *et al.* (2019) metabarcoding results, nevertheless the proportional read abundance values among NCM were low throughout our time-series (< 0.5%). We also observed that in November 2018 and April 2019 mixoplanktonic ciliate relative abundance exceeded 40% attaining maximum mixoplanktonic ciliate contribution to the community (**Figure 4.6**).

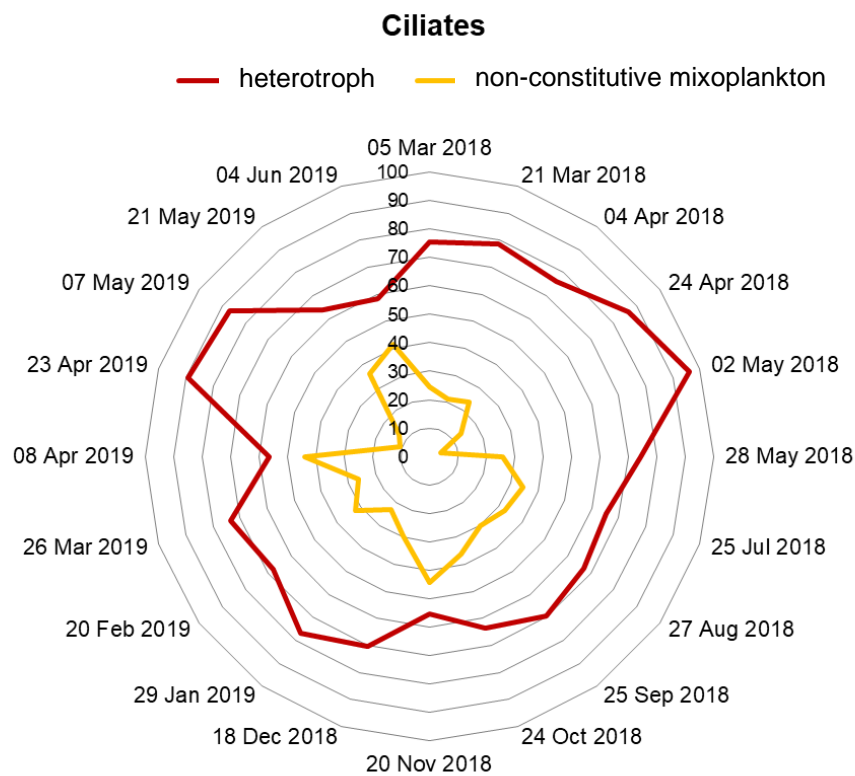


Figure 4.3 Radar chart displaying the temporal relative OTU reads proportions of major trophic modes (mixoplankton and heterotroph) in ciliates.

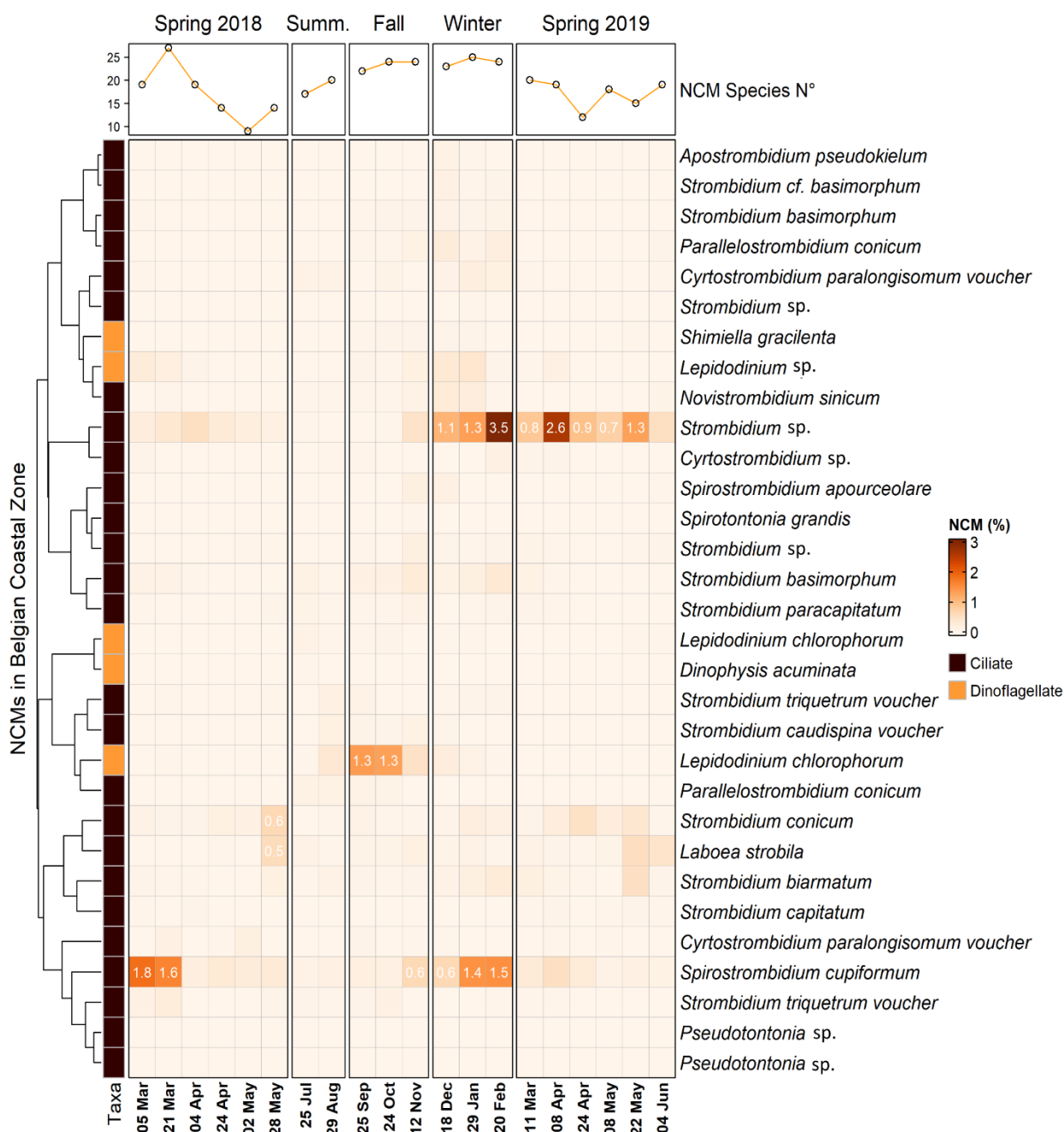


Figure 4.4 Series of seasonally arranged heatmaps displaying all the NCM protist occurring in the Belgian Coastal Zone time-series dataset (5 stations averaged). Line-plot above displays the temporal progression of the observed species richness at each time-point. Taxonomic affiliation of OTUs at the lowest possible level (species), is shown in lines. The colour scale (orange) represents the relative abundance contribution as percentage to the entire protistan community. Left annotation in colours refers to the taxa assigned for each of the species. The results that accounted > 0.5% of OTU reads were annotated. Row clustering and its corresponding dendrogram was built using Pearson distance.

4.3.2 NNS Summer 2018

In the NNS area, NCM had a low contribution to the protistan community, similar to BCZ time-series dataset, average = 3.1% (**Table 4.1**), whereas CM attained up to 51.0%. However, sites located most in the south of the BS transect, very close to the German coast (NS 1, NS a, NS b), showed the highest peaks of NCM relative abundances of the entire dataset (**Figure 4.6**). Indeed, *Lepidodinium chlorophorum* (two OTUs assigned) contributed up to 19.2% in site NS a. Northern sites (BS, SSF and NCZ) of BS transect were characterized by strong contributions of another NCM dinoflagellate, *Dinophysis acuminata* (**Figure 4.5**). In SSF and NCZ the tintinnid ciliate *Spirotontonia grandis* contributed substantially to the overall NCM weight, nevertheless *Lepidodinium chlorophorum* was still the most important contributor (**Figure 4.5**).

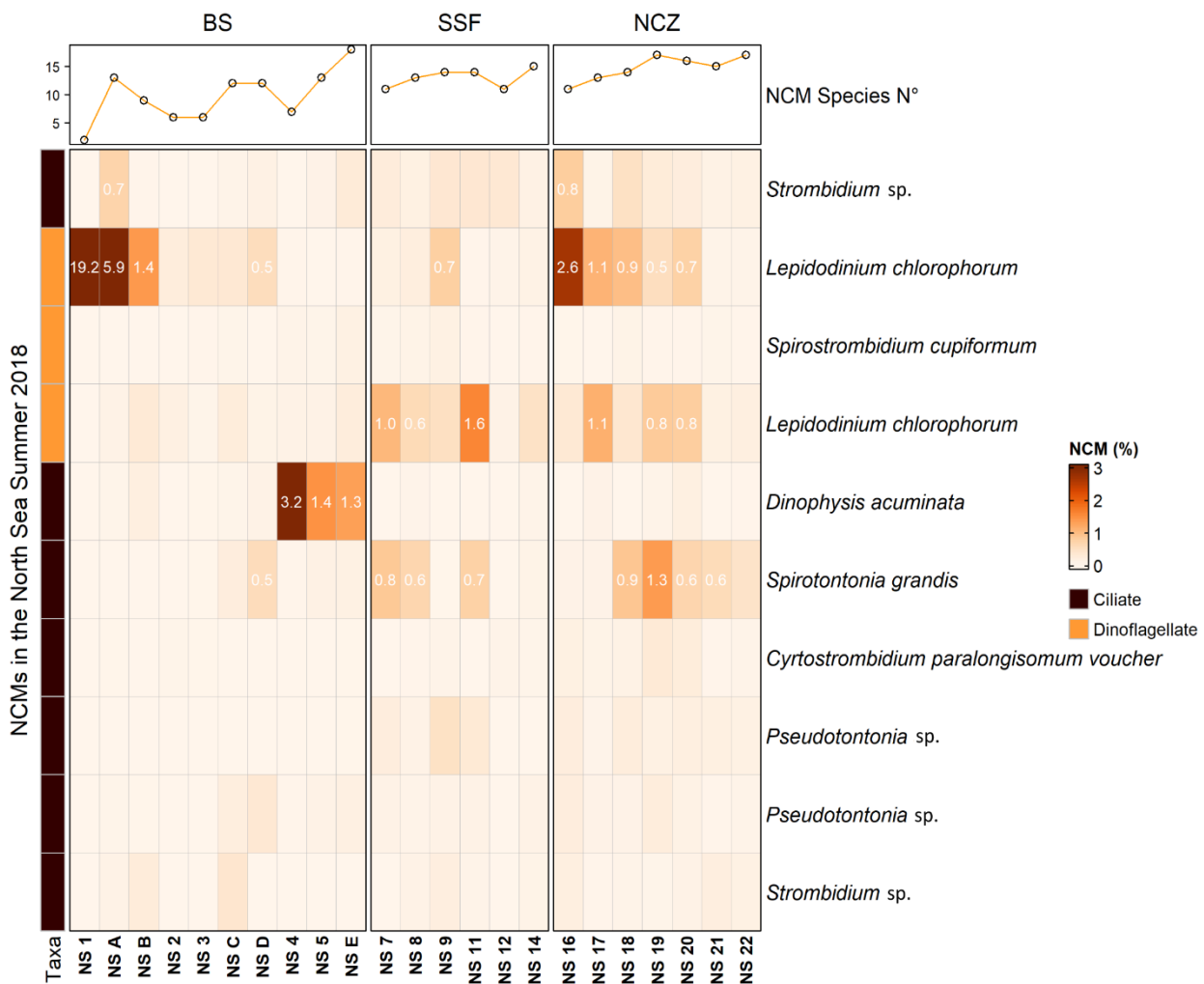


Figure 4.5 Series of geographically arranged heatmap per areas established displaying the top 10 most representative NCM in samples along the NNS samples collected in summer 2018. Line-plot above displays the temporal progression of the observed species richness at each sampling-point. Coloured stacked bar represent the proportions of reads of the different trophic strategies. Taxonomic affiliation of OTUs at the lowest possible level (species), is shown in lines. Left annotation in colours refers to the taxa assigned for each of the species. The colour scale (orange) represents the relative abundance calculated as percentage of final total reads per sample. The results that accounted > 0.5% of OTU reads are annotated.

4.3.3 Southern North Sea, May 2019

The SNS receives freshwater and nutrient loads from rivers (mainly the Seine and the Scheldt) that mix with inflowing English Channel waters. These nutrient enriched coastal systems are characterized by well-documented *Phaeocystis globosa* massive blooms that occur yearly as a single spring event lasting between 4-13 weeks (Breton *et al.*, 2006; Rousseau *et al.*, 2000) in high-nitrate but silicate-deficient conditions (Simó, 2001). Among the NCM detected (**Figure 4.6**), the ciliates belonging to *Strombidium* genus, were the only species that stood out on the dataset, particularly *Strombidium* sp. which attained noticeable high values in all the sites of the British Coast (ENG). Similarly, in the BCZ, only *Strombidium* sp. contributed > 0.5% to the community. Lowest NCM richness detected were in NL sites SS 51 and SS 49, located nearby Scheldt estuary (**Figure 4.6**).

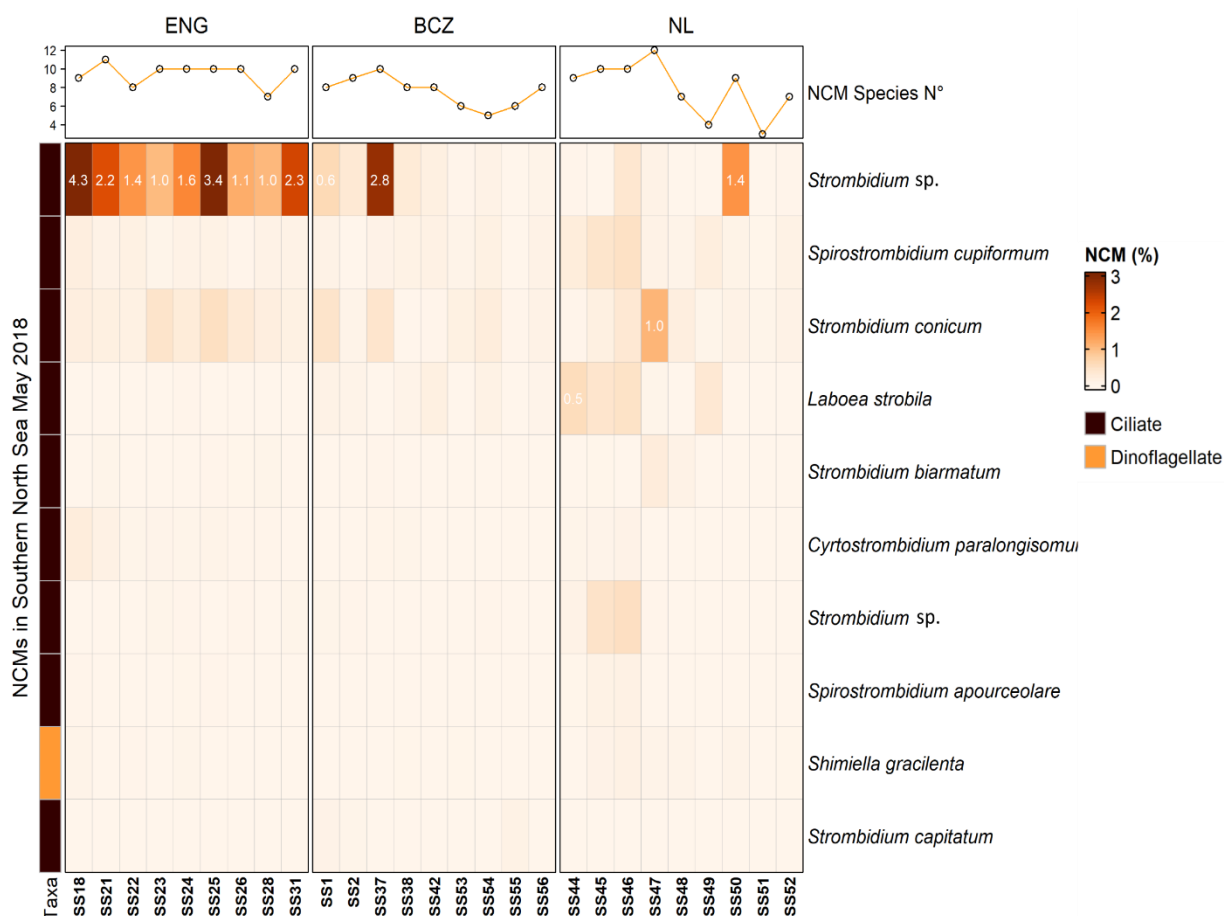


Figure 4.6 Series of geographically arranged heatmap per areas established displaying the top 10 most representative NCM in samples along the SNS samples collected in May 2019. Line-plot above displays the temporal progression of the observed species richness at each sampling-point. Coloured stacked bar represent the proportions of reads of the different trophic strategies. Taxonomic affiliation of OTUs at the lowest possible level (species), is shown in lines. Left annotation in colours refers to the taxa assigned for each of the species. The colour scale (orange) represents the relative abundance calculated as percentage of final total reads per sample. The results that accounted > 0.5% of OTU reads are annotated.

4.4 Discussion

We gathered new information on the spatial and temporal variability of NCM in the North Sea based on the analysis of 18S rRNA gene. On the three dataset subsets studied, the contribution of NCM to the taxonomic diversity of the entire eukaryotic protistan plankton (in terms of number of reads) was in general very scarce. In contrast, results showed that CM were present throughout the year, often dominating the community as previously revealed Schneider *et al.* (2020) for neighbouring areas, noting that the data in Schneider *et al.* excludes NCM other than *Mesodinium*.

Regarding the taxonomic composition of NCM, they were almost exclusively represented by oligotrich ciliate species, of which ~ 30% of OTU reads on average were identified as NCM; it has been shown that chloroplast-retaining oligotrichs rarely dominate the ciliate community (Dolan, 1992). Besides, various studies have demonstrated a low biomass of NCM throughout all year in temperate seas and in oligotrophic waters (Dolan and Pérez, 2000; Stoecker *et al.*, 2009; Romano *et al.*, 2021; Leles *et al.*, 2021).

In time-series, NCM mostly emerged in winter under conditions of high nutrients - low light, and the number of NCM species detected by metabarcoding was found to be lowest in April 2018 and May 2019 during *Phaeocystis globosa* blooms (data not shown). The datasets used for the spatial analysis showed that the contribution of NCM was considerably high (3.1% of OTU reads on average, **Table 4.1**) during the summer months in stratified waters of NNS, which are characterized by a permanent thermocline in the North Sea (Richardson *et al.*, 1998) that induces a sink of the colder and nutrient-rich waters away from the photic zone (Johns and Reid, 2001). Our approach was able to capture the post-*Phaeocystis* bloom period in SNS with high proportion of reads belonging to autotrophic organisms, and NCM presented very low contributions to the protistan community.

This work provides a first picture of the NCM temporal and spatial variability in the North Sea based on DNA metabarcoding. The major findings of this study are summarized as follows.

- (i) Marine oligotrich ciliates are major NCM contributors followed by few dinoflagellate species in the North Sea.
- (ii) NCM are minor contributors to the number of reads proportions of the entire protistan community throughout all year long.
- (iii) NCM species richness tend to increase beginning of summer and is maintained high until the end of the winter.
- (iv) NCM dinoflagellates such as *Lepidodinium chlorophorum* and *Dinophysis acuminata* were found to be more abundant (in number of reads) in stratified waters of the NNS summer.
- (v) In SNS, NCM contribution strongly decreases throughout the end phase of colonial *Phaeocystis* blooms, being *Strombidium sp.* most important contributor, particularly in ENG.

Our study did establish the presence of organisms that are known to be mixoplanktonic (NCM), however, that does not necessarily mean that they are actively performing photosynthesis or engaging in phagocytosis at a particular time and place.

5 Mediterranean oligotrophic waters: Subtropical waters

Filomena Romano & Paraskevi Pitta

5.1 Sampling

Sampling took place on a monthly basis from January to December 2019 at the coastal station POSEIDON-HCB (Heraklion Coastal Buoy, 35.426°N - 25.072°E, max depth 180 m), Heraklion Bay, Cretan Sea, Greece (**Figure 5.1**). Profiles of water column structure (temperature, salinity) and chl_a were performed with a Seabird CTD profiler equipped with a fluorescence sensor. Water samples were collected at seven depths in the euphotic zone (2, 10, 20, 50, 75, 100, 120 m) using 5 L Niskin bottles. Sampling was not performed in February and August due to bad weather at sea. Dissolved nutrient concentrations were assessed following Ivancic and Degobbis (1984) and Strickland and Parsons (1972) using a UV/VIS spectrophotometer with the detection limits for phosphate, ammonium, nitrate, nitrite and silicate being 0.018, 0.019, 0.017, 0.010 and 0.025 μM , respectively.

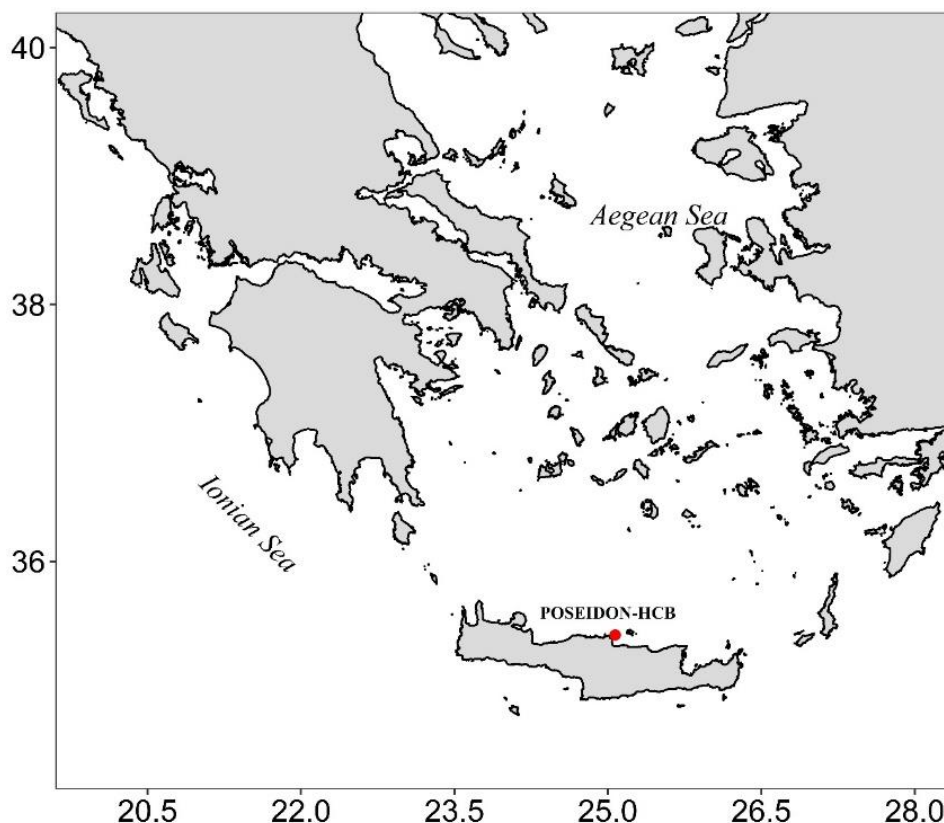


Figure 5.1 Map of the Sampling area in the Mediterranean Sea showing the position of the Poseidon-HCB station.

5.2 Materials and Methods

5.2.1 Ciliate abundance enumeration and biomass

For the enumeration and identification of ciliates, 250 mL of water were fixed with borax-buffered formalin (formaldehyde final concentration 2%) and stored at 4 °C in the dark. According to Stoecker *et al.* (1994), formaldehyde fixation may underestimate the total ciliate abundance by up to 65%. Acid Lugol's solution can give a higher estimation of cell abundance (Gifford, 1985) but does not allow the observation of the autofluorescence of chloroplasts. For this reason, the present study, focusing on trophic modes of ciliates (mixotrophy vs heterotrophy), reports results from samples fixed with formaldehyde. A parallel series of samples were fixed with 2% of acid Lugol's in order to estimate the percentage of cell loss and the correlation between abundances. One hundred mL of the sub-sample were concentrated using sedimentation chambers (Utermöhl, 1931) and cells were counted with an Olympus IX-70 inverted microscope equipped for transmitted light, phase-contrast and epifluorescence (blue light: DM 500 nm dichroic mirror, BP 420 to 480 nm exciter filter, BA 515 nm barrier filter and a 100 W mercury burner) at 150X magnification.

Oligotrichs and choreotrichs (both comprising aloricate species) were identified down to genus level in most of the cases and down to species level when possible, following Laval-Peuto (1986), Laval-Peuto & Rassoulzadegan (1988), Lynn *et al.* (1988), Montagnes *et al.* (1988), Lynn & Montagnes (1991). Those ciliates showing a homogeneous fluorescence were considered to be mixoplanktonic, while ciliates that did not show any fluorescence or specimens in which fluorescence was located in a specific part of the cell (probably food vacuole) were considered as heterotrophic. Tintinnids were identified based on the lorica shape and dimensions, after Jorgensen (1924) and Balech (1959). The dimensions of each individual cell were measured using an image analysis software (Image-Pro Plus 6.1). Aloricate ciliates were divided into four size classes based on their cell length. More specifically, the groups were identified as very small, small, medium, and large, referring, respectively, to cell length < 18, 18-30, 30-50, and > 50 µm. The biovolume was calculated using geometric shapes according to Peuto-Moreau (1991) and biomass by multiplying the biovolume with the conversion C factor of 0.14 pg C µm⁻³ used for samples fixed with 2% formaldehyde (Putt & Stoecker, 1989). For samples from January, we only report of total ciliate abundance due to a temporary malfunction of the image analysis system.

5.2.2 Statistical analysis

Two-way ANOVA (water column structure by depth) was used in order to reveal significant differences among samples grouped according to certain criteria (mixing/intermediate/stratification period and depth layers 2-120 m). This analysis was performed on four size classes (very small, small, medium, and large). In addition, two-way ANOVA (water column structure by month) was performed to test whether significant differences existed among samples grouped according to the mixing/intermediate/stratification period or certain months of the year; this analysis was performed on the mixotrophic ciliate genera.

Alpha diversity was measured temporally (for each month) and vertically (at each depth) using Shannon's H index, richness value and Pielou's Evenness index according to ciliate abundance. For the temporal evaluation of the alpha diversity, integrated values were used, while for the vertical evaluation, values of each depth were averaged (annual average). Rank abundance analysis was also carried out with R language version 4.0.1 and the integrated dataset, transformed using square root transformation, was used for temporal ranks, while annual average was used for vertical ranks.

5.3 Results

5.3.1 Temporal and vertical distribution

Throughout the water column, total abundance (cells L⁻¹) of mixoplanktonic ciliates represented $24 \pm 8.6\%$ of the pelagic ciliate community. In terms of vertical distribution, mixoplanktonic ciliates were abundant between 2 and 20 m depth; below this layer, their abundance decreased with depth (**Figure 5.2**).

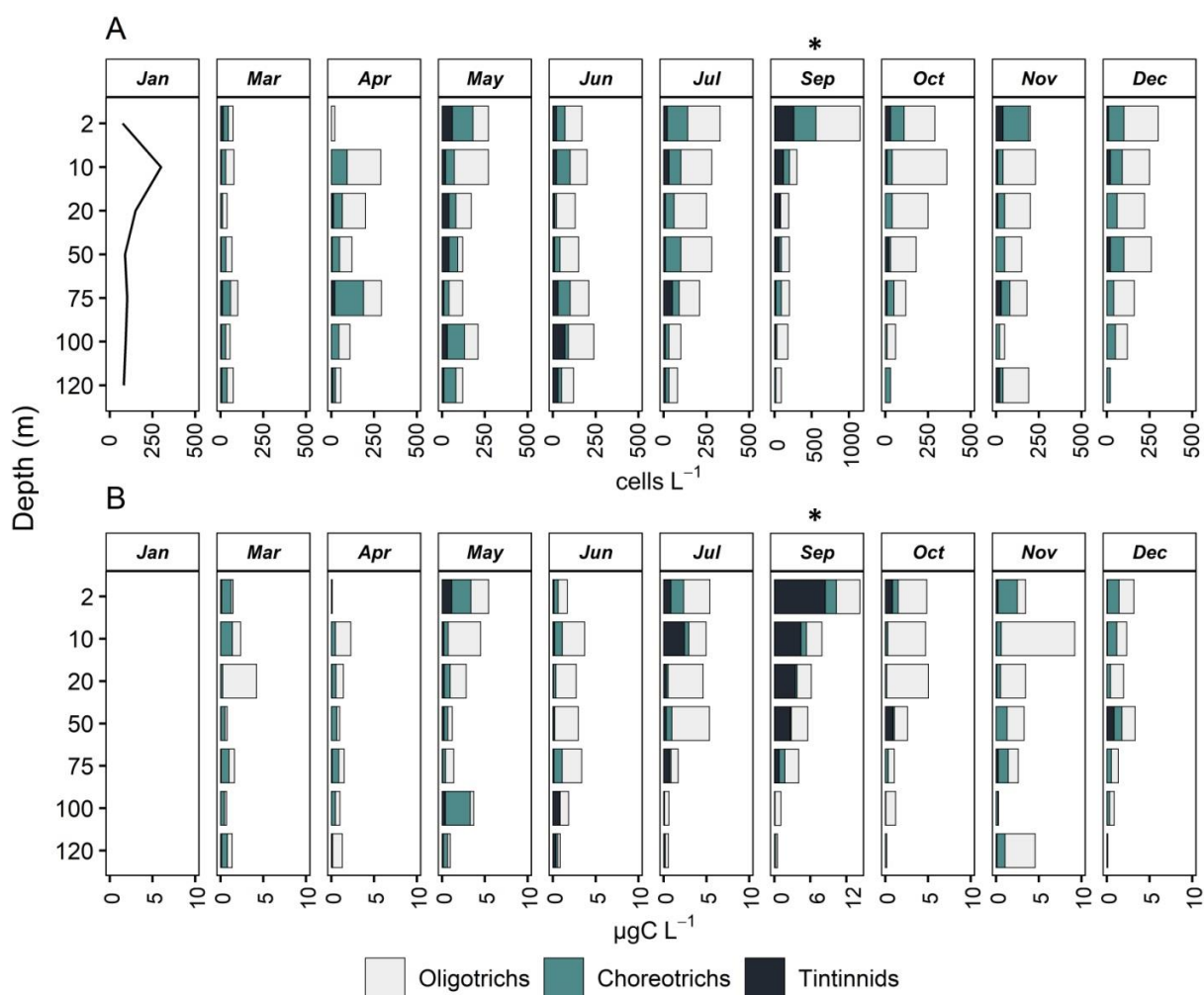


Figure 5.2. Vertical distribution of (A) abundance, cells L⁻¹ and (B) biomass, µg C L⁻¹ of oligotrichs, choreotrichs and tintinnids at all months sampled. For January, only total ciliate abundance is presented (line) and values for oligotrichs, choreotrichs and tintinnids are missing. Note that in September, the x axis has a different scale compared to all other months. (Romano *et al.* 2021). Mixoplanktonic ciliates are part of oligotrichs and the rest are heterotrophic.

This was true throughout the year, the only exception being June and July, which presented maxima at 100 and 50 m, respectively. Mixoplanktonic ciliates showed a very different vertical pattern compared to heterotrophic species that did not show any specific pattern and their distribution was not significantly correlated with depths (data not shown). In terms of integrated values (surface to 120 m), the abundance of mixoplanktonic ciliates ranged from 1.81×10^6 to 9.21×10^6 cells m^{-2} , while the integrated biomass ranged from 14 to 118 mg C m^{-2} . For both mixoplanktonic and heterotrophic species the lowest abundance was found in March and the highest in September and July, respectively (**Table 5.1**).

Table 5.1. Integrated values of abundance and biomass of mixoplanktonic and heterotrophic ciliates together with the maximum abundance at each depth. NA = not available. Numbers in parenthesis are depths of maximum abundance and biomass, respectively. See also Romano *et al.* (2021)

Month	Mixoplankton				Heterotrophs			
	Abundance	Biomass	Maximum abundance	Maximum biomass	Abundance	Biomass	Maximum abundance	Maximum biomass
	10^6 cells m^{-2}	mg C m^{-2}	Cells L^{-1} (m)	mg C L^{-1} (m)	10^6 cells m^{-2}	mg C m^{-2}	Cells L^{-1} (m)	mg C L^{-1} (m)
January	8.56	NA	142 (10)	NA	12.63	NA	192 (10)	NA
March	1.82	87	28 (10)	3.65 (20)	6.39	135.59	85 (75)	1.83 (10)
April	1.83	14	128 (10)	1.2 (10)	18.47	130.87	292 (75)	1.42 (75)
May	5.02	93	170 (10)	3.4 (10)	14.66	165.17	210 (2)	3.27 (2)
June	7.23	117	90 (100)	1.81 (10)	14.17	167.49	160 (75)	2.74 (75)
July	6.43	68	110 (50)	1.7 (50)	19.07	251.21	260 (2)	4.11 (2)
September	9.21	118	390 (2)	1.81 (10)	18.81	192.15	620 (2)	5.14 (2)
October	4.76	42	140 (10)	2.18 (50)	14.82	225.44	240 (2)	4.78 (20)
November	2.52	112	40 (10)	6.91 (10)	16.41	256.43	190 (10)	3.34 (120)
December	5.62	41	120 (2)	1.86 (2)	16.88	158.15	220 (50)	2.04 (50)

5.3.2 Size classes

In terms of size classes, the contribution values to the mixoplanktonic ciliate community were $4.26 \pm 3.05\%$, $10.55 \pm 3.52\%$, $5.79 \pm 2.20\%$, and $2.99 \pm 2.43\%$, while for biomass 0.67%, 4.02%, 7.03%, and 11.42%, respectively for ciliates < 18 or very small, 18-30 or small, 30-50 or medium and > 50 or large μm , respectively. During the stratification period (May to November), large (> 50 μm) mixoplanktonic cells were observed only above the DCM (at 50 m), while the deeper layers were populated by very small (< 18 μm) and small (18–30 μm) mixoplanktonic ciliates (**Figure 5.3**).

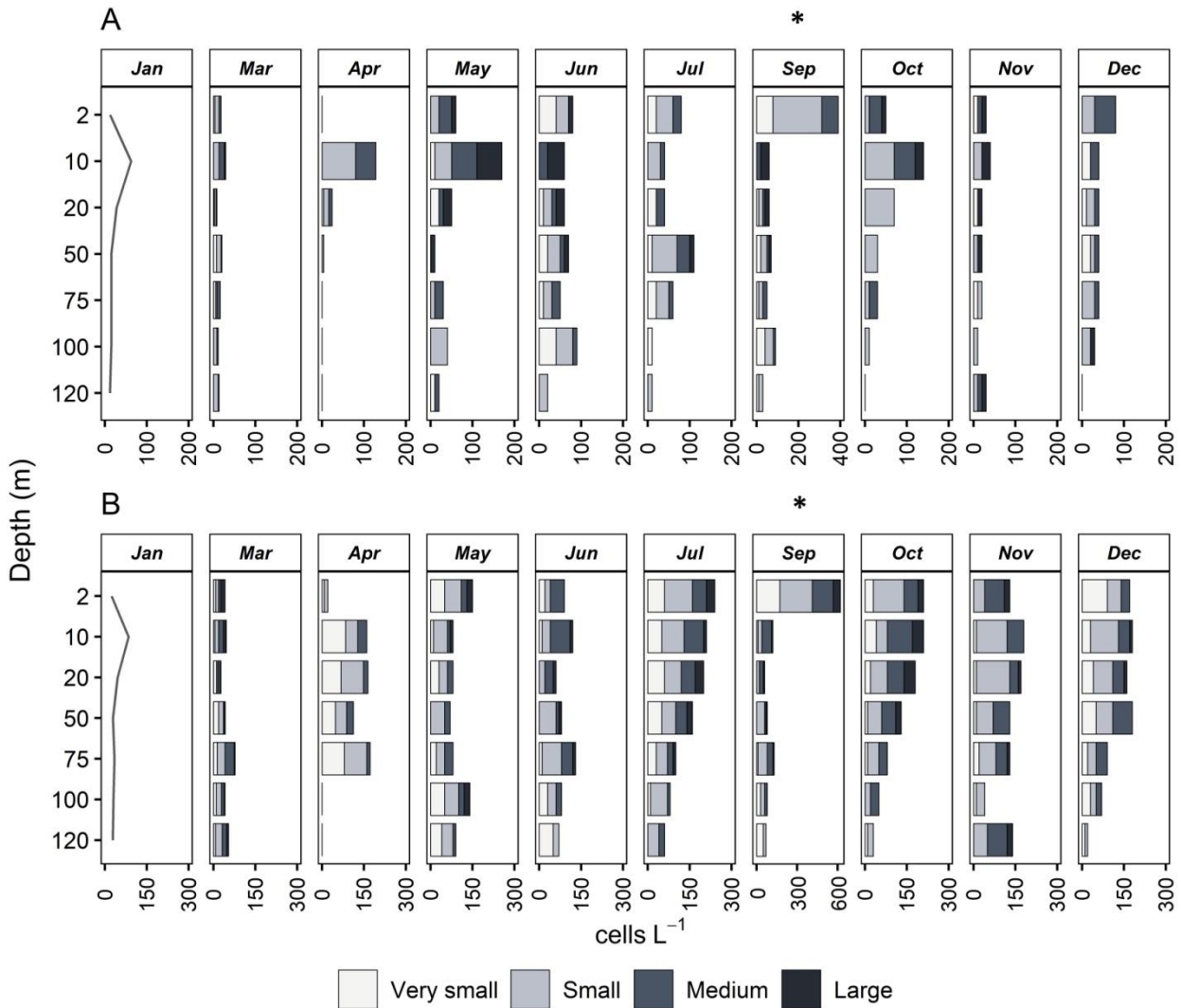


Figure 5.3 Vertical distribution of abundance (cells L⁻¹) of **(A)** four size classes of mixoplanktonic and **(B)** heterotrophic ciliates at all months sampled. Very small: < 18 μm, Small: 18-30 μm, Medium: 30-50 μm, Large: > 50 μm. Note that in September, the x axis has a different scale compared to all other months. See also Romano *et al.* (2021).

During the mixing period (December to May), mixoplanktonic species were very few, and the community was dominated especially by small and medium (18-30 μm, 30-50 μm) species. The integrated abundance of mixoplanktonic aloricates varied between 0 and 2.96 x 10⁶ cells m⁻² for very small, and between 0.91 and 3.41 x 10⁶ cells m⁻² for small species. When considering the integrated abundance of medium and large cells (30–50 and > 50 μm), mixoplanktonic ciliates were much lower numerically and varied between 0.16 and 1.80 x 10⁶ cells m⁻² for medium species and between 0.00 and 1.28 x 10⁶ cells m⁻² for large species (**Table 5.2**).

Table 5.2. Integrated abundance (10^6 cells m^{-2}) of four size classes of aloricate mixoplanktonic and heterotrophic ciliates at each month. Very small: $< 18 \mu m$, Small: $18-30 \mu m$, Medium: $30-50 \mu m$, Large: $>50 \mu m$. Minimum and maximum values are reported below and in the table. Maximum values are in bold and minimum values in italic.

Month	Mixoplankton				Heterotrophs			
	Very small	Small	Medium	Large	Very small	Small	Medium	Large
March	0.37	0.91	0.47	0.07	1.41	2.08	1.63	0.53
April	0.08	1.07	0.68	0.00	8.08	7.44	1.89	0.13
May	0.59	1.63	1.52	1.28	3.02	5.06	2.46	0.66
June	2.14	2.61	1.38	1.10	1.64	5.07	3.26	0.82
July	1.52	2.95	1.69	0.28	4.36	6.65	3.96	1.67
September	2.96	3.41	1.80	1.04	2.12	5.79	3.50	1.00
October	0.00	3.39	1.13	0.24	1.57	5.25	5.11	1.83
November	0.51	1.03	0.16	0.82	1.29	7.96	4.91	0.77
December	1.18	2.80	1.42	0.23	4.26	5.55	4.72	0.29
Max	2.96	3.41	1.80	1.28	8.08	7.96	5.11	1.83
Min	0.00	0.91	0.16	0.00	1.29	2.08	1.63	0.13

5.3.3 Genera of Mixoplanktonic Ciliates

The integrated abundances of mixoplanktonic ciliates were very low during autumn and spring, more specifically in October for very small species and November for medium cells, while the lowest number of small and large species was found in March and April, respectively. The integrated abundance of very small, small, medium and large, instead, was very high in June, October, July and May respectively.

Regarding mixoplanktonic ciliates, species/morphotypes of four genera were observed (*Strombidium*, *Tontonia*, *Laboea*, and the species *Mesodinium rubrum*). The temporal and vertical distribution of these four genera showed that *Strombidium* was the most abundant from all of them, which made up more than 50% of the total abundance. Plastidic specialist non-constitutive mixoplankton (pSNCM) as *Mesodinium rubrum* were abundant only in April. Mixoplanktonic species belonging to *Strombidium* and *Tontonia* genera were very abundant during June, July, and September when the stratification was well formed. Mixoplanktonic *Strombidium* species that were abundant during the stratification period belonged to the very small and small size classes (**Figure 5.4**).

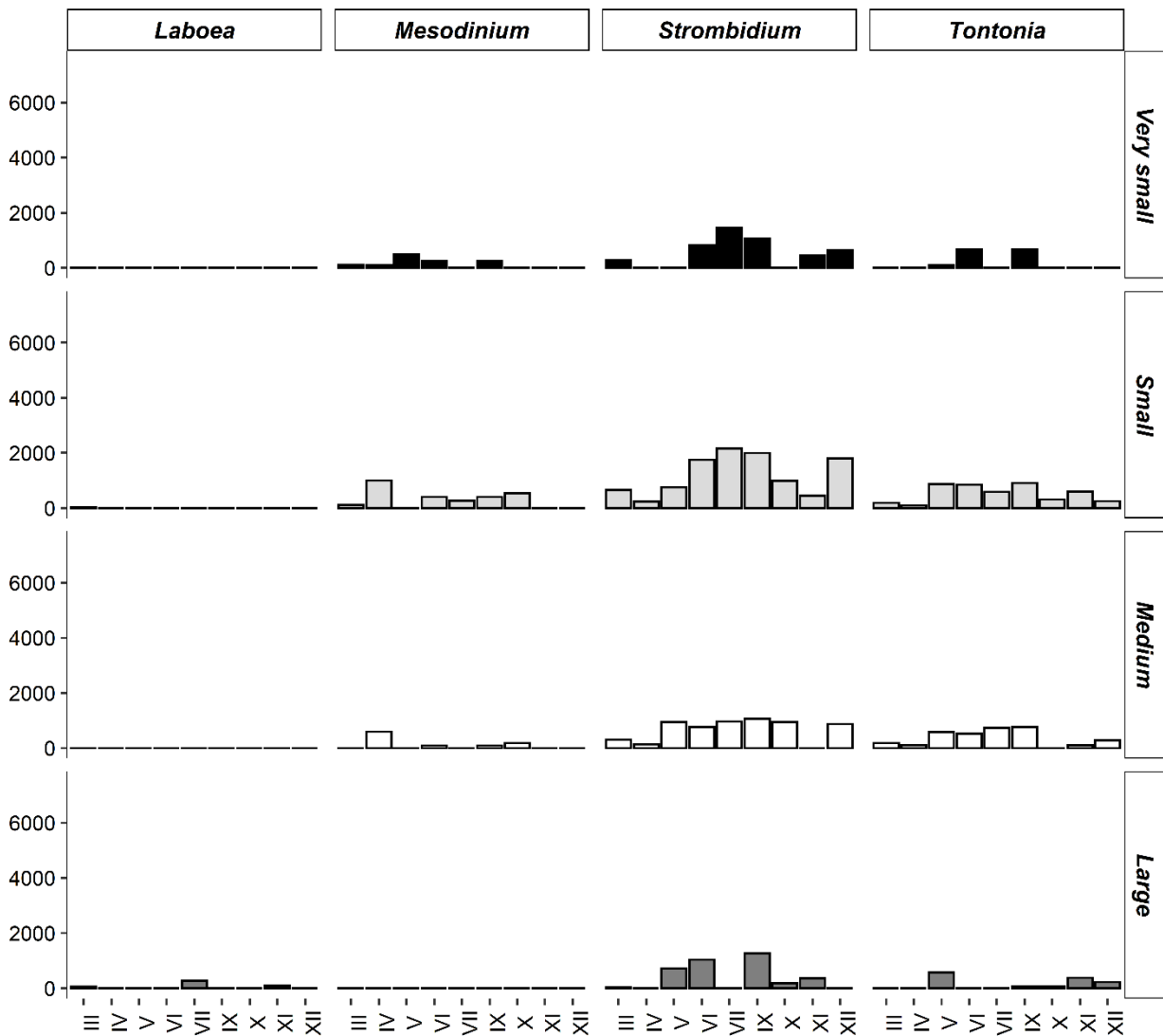


Figure 5.4 Depth-integrated abundance (cells m⁻²) of four size classes of mixoplanktonic genera of ciliates at all months sampled. Very small: <18 μm, Small: 18-30 μm, Medium: 30-50 μm, Large: >50 μm. See also Romano *et al.* (2021).

5.3.4 Alpha diversity

From the rank abundance curve analysis for each depth, the most abundant species, in terms of cells L⁻¹, belong to *Strombidium* genus, except for 100 m where the most abundant genus was *Leegaardiella*. The most abundant species were *Strombidium acutum* and *S. conicum* for 2, 10 and 20 m, while *S. epidemum* dominated the water column at 50, 75 and 120 m. *Strombidium acutum* and *S. conicum* are two mixoplanktonic microciliates, and they are the most abundant species at the surface of the water column. For this reason, it is possible that these two species contributed for the most of the mixoplanktonic microciliates (>30 μm) biomass at the surface layer. *Strombidium epidemum*, on the other hand, contributed for the most of heterotrophic very small ciliate biomass at 75 m (**Figure 5.5**).

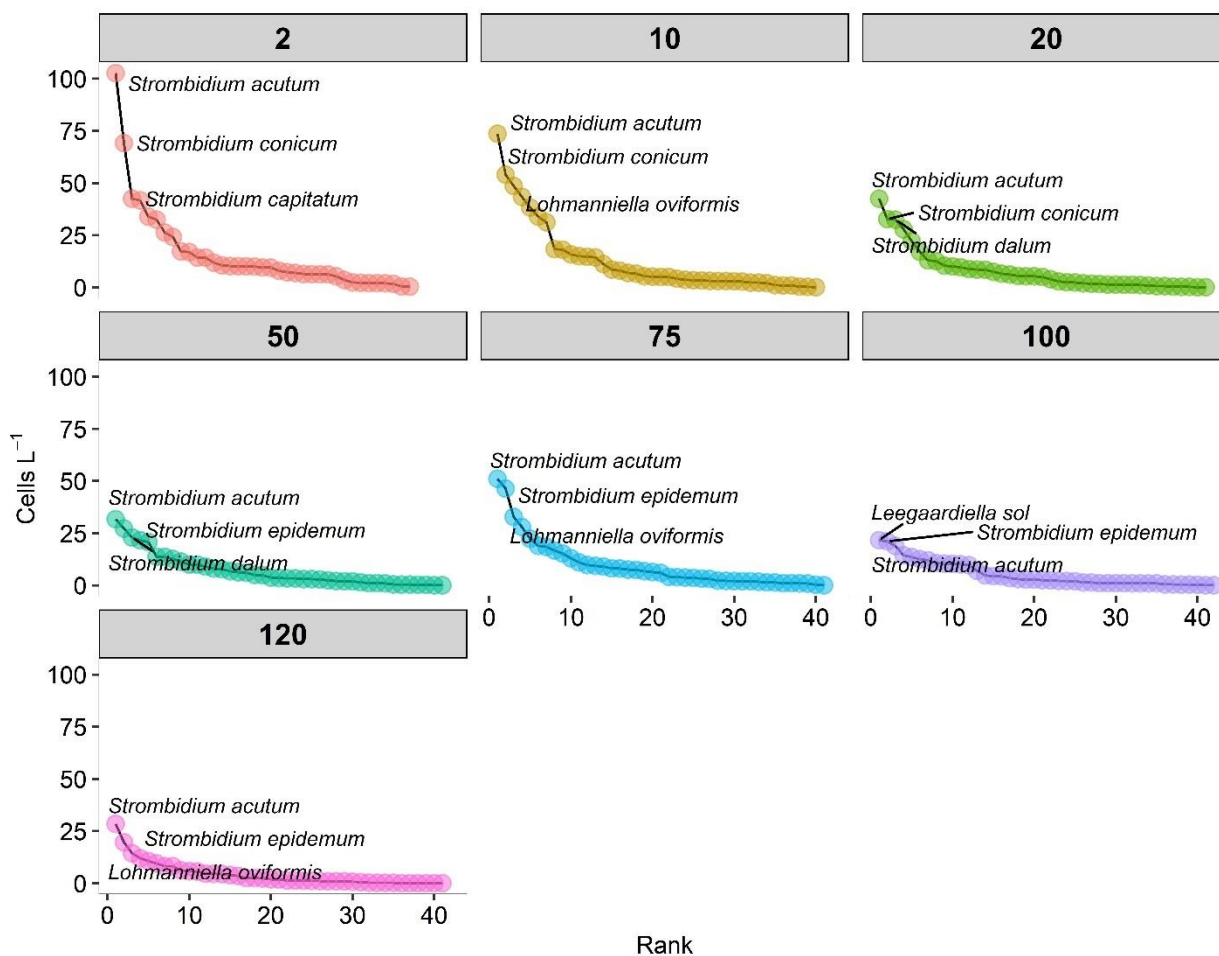


Figure 5.5. Rank abundance curve of annual average of ciliate abundance at each depth. Only the names of the first two most abundant species are reported here. *Strombidium acutum*, *S. conicum*, and *S. capitatum* are mixoplanktonic.

Table 5.3 Correlation between biomass of mixoplanktonic (mix) and heterotrophic (het) ciliates smaller and bigger than $30 \mu\text{m}$ with abiotic factors. Significant p values are in green. Ns = not significant.

	Het < 30 μm		Mix < 30 μm		Het > 30 μm		Mix > 30 μm	
	R	p	R	p	R	P	R	p
Temperature	-0.05	ns	0.20	ns	0.64	0.00	0.31	0.02
Salinity	0.08	ns	0.15	ns	0.25	Ns	0.19	ns
DIN	-0.09	ns	-0.23	ns	-0.47	0.00	-0.37	0.00
PO₄³⁻	-0.03	ns	-0.15	ns	-0.28	0.03	-0.13	ns
SiO₄³⁻	0.28	0.03	0.07	ns	-0.16	Ns	-0.14	ns
Chla	0.20	ns	-0.12	ns	-0.19	Ns	-0.08	ns

From the correlation analysis, only the biomass of heterotrophic very small ciliates is significantly positive with SiO_4 , while bigger ciliates are significantly correlated with the temperature and negatively correlated with DIN. Very small mixoplanktonic ciliates did not show any significant correlation with any abiotic factor (**Table 5.3**).

Rank abundance analysis was conducted on numerical integrated abundance of planktonic ciliate species. The results showed that most of the months belonging to the mixed water period (**Figure 5.5**) are mostly very diverse and no clear dominance was detected. During stratification, June and September showed that some species were more dominant compared to the others. More specifically, *Strombidium acutum* and *S. dalum* abundances were two times higher than other species abundances (**Figure 5.5**). *Strombidium* was the most dominant genus in all months except for March and October where the genera that dominated the community were *Lohmanniella* and *Pelagostrobilidium*, respectively.

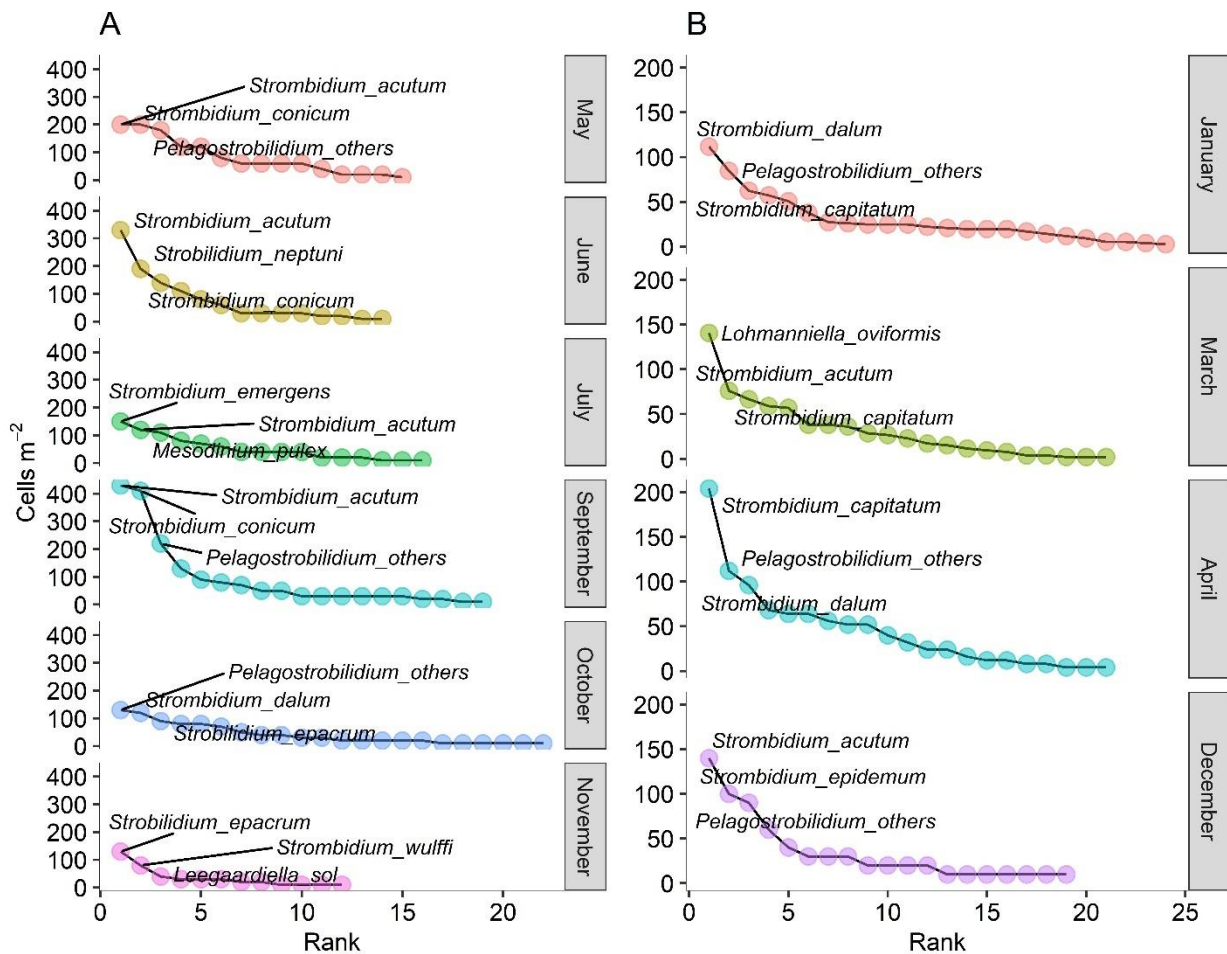


Figure 5.6. Rank abundance analysis of pelagic ciliate species during stratified (A) and mixed (B) water. Only the names of the first two most abundant species are reported here. *Strombidium acutum*, *S. conicum*, *S. dalum* and *S. capitatum* are mixoplanktonic.

Shannon index H' , species richness and Pielou's evenness were calculated for the integrated abundance of pelagic ciliates at each month sampled and the annual average at each depth. The biodiversity analysis conducted at each month showed that September had the highest Shannon index while the lowest values were found in April, November, and December. The values for the other months ranged between 2.8 and 3.0. January showed the highest value but the lowest regarding the Evenness. On the other hand, October and May showed very low value of species richness but a high value of Evenness (**Figure 5.6**).

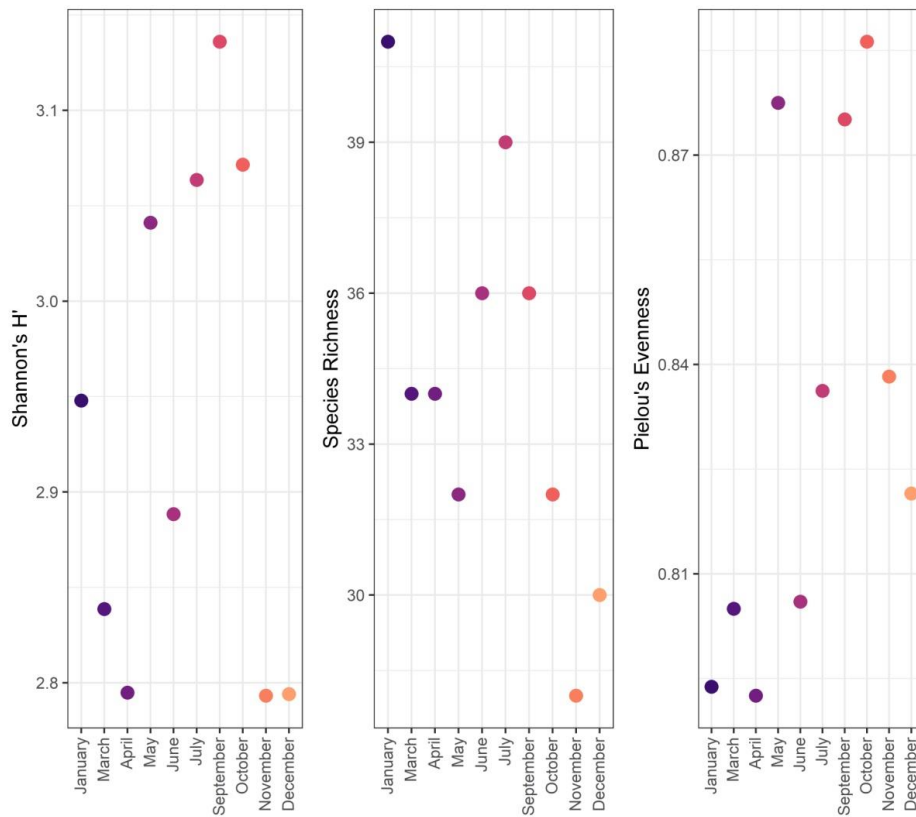


Figure 5.7 Shannon's H, species richness and Pielou's Evenness values at each month sampled for the integrated abundance of planktonic ciliates. The coloured symbols represent different months.

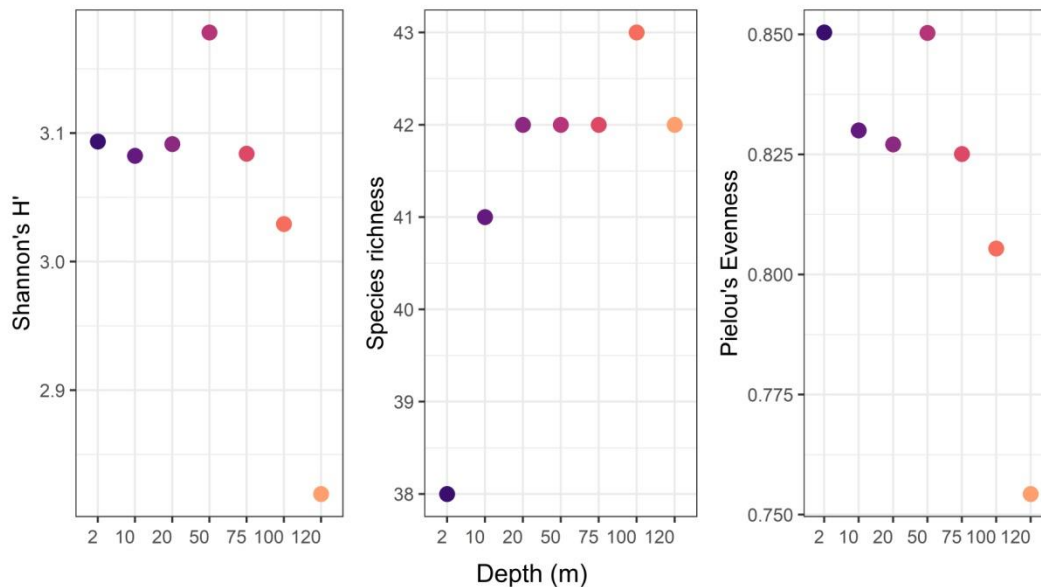


Figure 5.8 Shannon's H, species richness and Pielou's Evenness at each depth for the annual average of planktonic ciliates. The coloured symbols represent different months.

Regarding the annual average at each depth, Shannon's H index value was in the same range except for 50 m and 120 m that showed the highest and the lowest value

respectively. Between 2 and 20 m species richness increased exponentially while it remained stable down to the bottom (120 m) with the highest value at 100 m. On the other hand, Evenness decreased with depths except for 2 and 50 m that showed the highest values. More specifically, those indices showed that the surface was populated by few species and the abundance was homogenous, but in the bottom the number of species increased and a strong dominance of some species compared to the others (**Figures 5.7 and 5.8**).

5.4 Discussion

Consistent with, and building from, previous studies (Pitta & Giannakourou, 2000; Pitta *et al.*, 2001), mixoplanktonic ciliates were found to widely populate this oligotrophic environment, which is poor in nutrients but with plenty of light. The data presented here showed that planktonic ciliates of different types of trophic strategies displayed different vertical and temporal distributions, relative to the season. Heterotrophic ciliate abundance and biomass did not show any seasonality but were closely linked to chl_a concentration. In contrast, mixoplanktonic forms were largely restricted to the months with high temperatures and light. In the near-surface samples, mixoplanktonic species formed an important part of total ciliate abundance and biomass, and likely moved to deeper layers during June and July. If we consider size classes, large mixoplanktonic species were found only above DCM, while small and very small mixoplankton were present throughout the water column. Since it is known that oligotrophic conditions favour nanoplankton feeding on pico-bacterioplankton in tropical and temperate areas (Zubkov & Tarran, 2008), if we report on trophic relationships from oligotrophic environments, nano-ciliates (very small <18 µm) should also be considered because they represent an important grazer (except for nano-flagellates) for picoplankton.

This is one of few studies reporting on the annual dynamics and vertical distribution of size classes of mixoplanktonic vs heterotrophic ciliates through the water column (2-120 m), taking into account the contribution of the very small and small (<30 µm) mixoplanktonic ciliates that were found to comprise up to 50% of the total ciliate community during June, July, and September (a significantly different abundance between the stratification and mixing periods), most probably grazing on bacterioplankton and pico-phytoplankton that flourish during the stratification compared to the mixing period. Larger mixoplankton, like *Laboea strobila* and *Tontonia appendiculariformis*, were found only during the construction and destruction of the water column stratification (May and November, respectively; a significantly different abundance was found between the mixing and intermediate periods).

Based on these results, we may conclude that the four size classes of NCM (very small, small, medium, and large) have distinct vertical distributions throughout the water column, reflecting different ecological strategies. Due to their limited size (< 18 µm), very small ciliates feed only on picoplankton (bacteria, cyanobacteria, and flagellates) so they could be considered generalists since those groups are present through the whole water column. Larger mixoplankton (> 50 µm) are probably more specialists since they can feed only on some groups belonging to phytoplankton. This could explain the differences in the vertical distribution of the four size classes of mixoplanktonic ciliates.

6 Conclusions

For the first time, we gathered knowledge of the spatial, vertical and temporal variability of GNCM and pSNCM in three different marine environments (Arctic waters, North Sea, Mediterranean Sea) and using two different methodological approaches. The composition of Arctic and Mediterranean coastal water NCM communities was assessed using optical methods whereas the North Sea's communities were studied using DNA-based approaches. Microscopy provides high quality quantitative data but lacks high taxonomic resolution. In contrast DNA metabarcoding, provides only semi-quantitative information usually with biases, but with higher taxonomic resolution.

The contribution of NCM to total protist plankton is greatest during stratified periods in Arctic, temperate and tropical waters, characterized by high solar radiation and low inorganic nutrient concentrations. In tropical waters that see year-round stratification in the water column, and are generally nutrient limited, pSNCM are often restricted to shallow coastal waters while GNCM were found to comprise up to ~70% of the ciliate assemblages in offshore surface waters (Canals *et al.*, 2020). One may argue that this difference is due to pSNCM relying more heavily on photosynthesis (Hansen *et al.*, 2013), while GNCM are not directly affected by the inorganic nutrient limitations that restricts phototrophic growth and/or by the unavailability of specific prey. However, it should be noted that GNCM depend critically upon phototrophic prey which are subjected to such nutrient limitations.

In the sub-tropical, stratified, summer waters of the Mediterranean Sea, mixoplankton species have been found in abundance throughout nutrient-deficient surface layers, as well as in deeper waters at and under the deep chlorophyll maxima (Dolan and Marrasé, 1995; Dolan *et al.*, 1999). Throughout the vertical stratification, mixoplankton exhibit an increased relative importance in areas where phytoplankton biomass is lower, likely due to their ability to utilize inorganic carbon fixation to increase gross growth efficiency (GGE) and prolong survival in prey-starved environments. GNCM in particular can sometimes account for up to 100% of ciliate biomass in the photic zone, though the average annual contribution of GNCM to ciliate biomass is generally between 40-50%, often achieving peak values in spring and autumn. pSNCM ciliates (represented by the red *Mesodinium* spp.), however, are relatively rare in the Mediterranean Sea, with peak abundances when and where dissolved nutrient concentrations are highest. They (i.e., pSNCM) represent an average of just 3-9% of annual ciliate biomass (Bernard and Rassoulzadegan, 1994; Modigh, 2001).

The trend of increasing seasonal variation with increasing latitude continues into the more extreme temperate and polar climates where vertical stratification dissipates and light becomes limiting in the winter months, inhibiting primary production. Interestingly, both GNCM and pSNCM ciliates are often recorded, albeit at low levels, throughout the darkness of winter (Haraguchi *et al.*, 2018; Stoecker and Lavrentyev, 2018). This appears to contradict laboratory findings that suggest GNCM will die within days to weeks without sufficient prey. Some suggestions of how these plankton may survive over winter have been discussed, including decreased winter metabolism, cyst formation, and exploitation of patchy food sources (Levinsen *et al.*, 2000). In early spring, however, light returns, temperature increases, ice melts, and waters become stratified, giving photosynthetic

organisms the ability to take advantage of the winter-long nutrient regeneration. In temperate and polar surface waters, pSNCM often bloom in spring, reaching levels nearly 20 times greater than recorded at more southern latitudes (Leles *et al.*, 2017). Generally, GNCM bloom 1-3 months later than pSNCM, but maintain significant biomass well into the summer months when SNCM populations crash as nutrient concentrations become depleted in the euphotic zone. Indeed, GNCM generally see the greatest relative contribution to ciliate biomass in summer-time surface waters of both temperate and polar climates, reaching up to 85-90%.

Both GNCM and pSNCM spring/summer blooms tend to occur later in polar climates than in temperate climates (Levinsen *et al.*, 2000; Haraguchi *et al.*, 2018). As the deep chlorophyll maximum deepens into summer months, GNCM have been shown to be able to maintain biomasses here comparable to those found at surface waters (Levinsen *et al.*, 2000), and GNCM can contribute up to 46% of the chlorophyll-a found at the deep chlorophyll maxima (Franzè and Lavrentyev, 2017). Even at depths below the euphotic zone, GNCM ciliates can thrive presumably due to their ability to function as completely heterotrophic organisms. In fact, at and below the depth of the chlorophyll maxima, where light is so low that it may strongly limit photosynthesis, GNCM organisms exhibit patterns similar to their heterotrophic counterparts, and experience less seasonal variability than in well-lit surface waters (Levinsen *et al.*, 2000).

NCM are a pivotal link between the nano-size primary producers and higher trophic levels. The ability to couple an acquired ability to photosynthesize with phagotrophy can give all NCM a competitive advantage over pure phototrophs or heterotrophs, and would likely booster the trophic transfer in specific environments and seasons. However, inclusion of NCM as separate functional groups in biomass-based ecosystems models requires suitable field data (as done by Leles *et al.*, 2018, 2021). Challenges are related to identification of these organisms in field samples, because of their fragility, and because taxonomy is not often associated to a trophic description. In surveys based on morphological identification, special care must be taken during the collection of samples and transparent fixatives should be used in conjunction with the traditional Lugol's solution. When molecular techniques are employed, updated literature should be examined to classify organisms based on their trophic mode. The main challenge in survey protocols, however, lies on the standardization of an analytical pipeline where samples can be processed by both approaches and their results combined.

7 References

- Andersen P, Kristensen HS (1995) Rapid and precise identification and counting of thecate dinoflagellates using epifluorescence microscopy. In *Harmful Marine Algal Blooms Eds.* Lassus PG, Arzul P, Gentian P, Marcaillou P pp:713-718.
- Arendt KE, Nielsen TG, Rysgaard S, Tønnesson K (2010) Differences in plankton community structure along the Godthåbsfjord, from the Greenland Ice Sheet to offshore waters. *Mar. Ecol. Prog. Ser.* **401**: 49–62. doi:10.3354/meps08368.
- Arendt KE, Agersted MD, Sejr MK, Juul-Pedersen T (2016) Glacial meltwater influences on plankton community structure and the importance of top-down control (of primary production) in a NE Greenland fjord. *Estuar. Coast. Shelf Sci.* **183**:123–135. doi:10.1016/j.ecss.2016.08.026.
- Balech E (1959) *Tintinnoinea del Mediterraneo*. Trabajo Instituto Espanol de Oceanografia **28**: 1–88.
- Bernard C, Rassoulzadegan F (1994) Seasonal variations of mixotrophic ciliates in the northwest Mediterranean Sea. *Mar. Ecol. Prog. Ser.* **108**: 295–302. <https://doi.org/10.3354/meps108295>
- Breton E, Rousseau V, Parent JY, Ozer J, Lancelot C (2006) Hydroclimatic modulation of diatom/*Phaeocystis* blooms in nutrient-enriched Belgian coastal waters (North Sea). *Limnol. Oceanogr.* **51**:1401–1409.
- Burkholder JAM, Glibert PM, Skelton HM (2008) Mixotrophy, a major mode of nutrition for harmful algal species in eutrophic waters. *Harmful Algae* **8**: 77–93.
- Canals O, Obiol A, Muhovic I, Vaqué D, Massana R (2020) Ciliate diversity and distribution across horizontal and vertical scales in the open ocean. *Mol. Ecol.* **29**: 2824–2839.
- Chain FJJ, Brown EA, Macisaac HJ, Cristescu ME (2016) Metabarcoding reveals strong spatial structure and temporal turnover of zooplankton communities among marine and freshwater ports. *Divers. Distrib.* **22**: 493–504.
- Crawford D (1989) *Mesodinium rubrum*: the phytoplankter that wasn't. *Mar. Ecol. Prog. Ser.* **58**: 161–174.
- Desmit X, Ruddick K, Lacroix G (2015) Salinity predicts the distribution of chlorophyll a spring peak in the southern North Sea continental waters. *J. Sea Res.* **103**: 59–74.
- Dolan JR (1992) Mixotrophy in ciliates: a review of *Chlorella* symbiosis and chloroplast retention. *Mar. Microb. Foodwebs* **6**: 115–132.
- Dolan JR, Marrasé C (1995) Planktonic ciliate distribution relative to a deep chlorophyll maximum: Catalan Sea, N.W. Mediterranean, June 1993. *Deep. Sea Res. Part I* **42**: 1965–1987.
- Dolan JR, Pérez MT (2000) Costs, benefits and characteristics of mixotrophy in marine oligotrichs. *Freshw. Biol.* **45**: 227–238.

- Dolan JR, Vidussi F, Claustre H (1999) Planktonic ciliates in the Mediterranean Sea: Longitudinal trends. *Deep. Sea Res. Part I* **46**: 2025–2039.
- Ducrotoy J-P, Elliott M, de Jonge VN (2000) The North Sea. *Mar. Pollut. Bull.* **41**: 5–23.
- Faure E, Not F, Benoiston AS, Labadie K, Bittner L, Ayata SD (2019) Mixotrophic protists display contrasted biogeographies in the global ocean. *ISME J.* **13**: 1072–1083.
- Flynn KJ, Stoecker DK, Mitra A, Raven JA, Glibert PM, Hansen PJ, Granéli E, Burkholder, JM (2013) Misuse of the phytoplankton–zooplankton dichotomy: the need to assign organisms as mixotrophs within plankton functional types. *J Plankton Res* **35**: 3-11.
- Flynn KJ, Mitra A, Anestis K, Anschütz A, Calbet A, Ferreira GD, Gypens N, Hansen PJ, John U, Lapeyra J, Mansour J, Maselli M, Medic N, Norlin A, Not F, Pitta P, Romano F, Saiz, E., Schneider L, Stolte W, Traboni C (2019). Mixotrophic protists and a new paradigm for marine ecology: where does plankton research go now? *J. Plankton Res.* **41**: 375–391.
- Franzè, G., Lavrentyev, P.J. (2017). Microbial food web structure and dynamics across a natural temperature gradient in a productive polar shelf system. *Mar. Ecol. Prog. Ser.* **569**: 89–102.
- Gifford, D. (1985). Laboratory culture of marine planktonic oligotrichs (Ciliophora, Oligotrichida). *Mar. Ecol. Prog. Ser.* **23**: 257–267.
- Gran-Stadniczeňko, S., Egge, E., Hostyeva, V., Logares, R., Eikrem, W., Edvardsen, B. (2019). Protist diversity and seasonal dynamics in Skagerrak plankton communities as revealed by metabarcoding and microscopy. *J. Eukaryot. Microbiol.* **66** : 494–513.
- Gypens, N., Lacroix, G., Lancelot, C. (2007). Causes of variability in diatom and *Phaeocystis* blooms in Belgian coastal waters between 1989 and 2003: A model study. *J. Sea Res.* **57**: 19–35.
- Hansen, P. J., Calado, A. J. (1999). Phagotrophic mechanisms and prey selection in free-living dinoflagellates. *J. Eukaryot. Microbiol.* **46**: 382–389.
- Hansen, P.J., Tillmann, U. (2020). *Mixotrophy among dinoflagellates – prey selection, physiology and ecological importance*. In: Subba Rao Durvasula (Ed). *Dinoflagellates: Classification, Evolution, and Ecological Significance*. Nova Science Publishers, Inc, p. 201-260
- Hansen, P. J., Nielsen, L. T., Johnson, M., Berge, T., Flynn, K. J. (2013). Acquired phototrophy in *Mesodinium* and *Dinophysis* - A review of cellular organization, prey selectivity, nutrient uptake and bioenergetics. *Harmful Algae* **28**: 126–139.
- Haraguchi L, Jakobsen HH, Lundholm N, Carstensen J (2018). Phytoplankton community dynamic : A driver for ciliate trophic strategies. *Front. Mar. Sci.* **5**: 272.
- Hillebrand H, Dürselen CD, Kirschtel D, Pollinger U, Zohary T (1999). Biovolume calculation for pelagic and benthic microalgae. *J. Phycol.* **35**: 403–424.

- Holding JM, Markager S, Juul-Pedersen T, Paulsen ML, Møller EF, Meire L, Sejr MK (2019). Seasonal and spatial patterns of primary production in a high-latitude fjord affected by Greenland Ice Sheet run-off. *Biogeosciences* **16**: 3777–3792.
- Hopwood MJ, Carroll D, Dunse T, Hodson A, Holding JM, Iriarte JL, *et al.* (2020). Review article: How does glacier discharge affect marine biogeochemistry and primary production in the Arctic? *Cryosphere* **14**: 1347–1383.
- Ivancic I, Degobbis D (1984). An optimal manual procedure for ammonia analysis in natural waters by the indophenol blue method. *Water Res.* **18**: 1143–1147.
- Jacobson DM, Anderson DM (1986). Thecate heterotrophic dinoflagellates: feeding behavior and mechanisms. *J. Phycol.* **22**: 249–258.
- Jonsson PR (1986). Particle size selection, feeding rates and growth dynamics of marine planktonic oligotrichous ciliates (Ciliophora: Oligotrichina). *Mar. Ecol. Prog. Ser.* **33**: 265–277.
- Jørgensen EG (1924). Mediterranean Tintinnidae. Report on the Danish oceanographical expedition 1908–1910 to the Mediterranean and adjacent seas. Copenhagen. 2. J.3 (Biology).
- Kim M, Drumm K, Daugbjerg N, Hansen PJ (2017). Dynamics of sequestered cryptophyte nuclei in *Mesodinium rubrum* during starvation and refeeding. *Front. Microbiol.* **8**: 1–14.
- Krawczyk DW, Witkowski A, Juul-Pedersen T, Arendt KE, Mortensen J, Rysgaard S (2015). Microplankton succession in a SW Greenland tidewater glacial fjord influenced by coastal inflows and run-off from the Greenland Ice Sheet. *Polar Biol.* **38**: 1515–1533.
- Lancelot C, Spitz Y, Gypens N, Ruddick K, Becquevort S, Rousseau V, Lacroix B, Gillen B (2005). Modelling diatom and *Phaeocystis* blooms and nutrient cycles in the Southern Bight of the North Sea: The MIRO model. *Mar. Ecol. Prog. Ser.* **289**: 63–78.
- Laval-Peuto M (1986). On plastid symbiosis in *Tontonia appendiculariformis* (Ciliophora, Oligotrichina). *BioSystems* **19**: 137–158.
- Laval-Peuto M, Rassoulzadegan F. (1988). Autofluorescence of marine planktonic Oligotrichina and other ciliates. *Hydrobiologia*, **159**: 99–110.
- Leles SG, Mitra A, Flynn KJ, Stoecker DK, Hansen PJ, Calbet A, McManus GB, Sanders RW, Caron DA, Not F, Hallegraeff GM, Pitta P, Raven JA, Johnson MD, Glibert PM, Våge S (2017). Oceanic protists with different forms of acquired phototrophy display contrasting biogeographies and abundance. *Proc. R. Soc. B* **284**: 20170664.
- Leles SG, Polimene L, Bruggeman J, Blackford J, Ciavatta S, Mitra A, Flynn KJ (2018) Modelling mixotrophic functional diversity and implications for ecosystem function. *J. Plankton Res.* **40**: 627-642.
- Leles SG, Mitra A, Flynn KJ, Tillmann U, Stoecker DK, Jeong HJ, Burkholder JM, Hansen PJ, Caron D, Glibert PM, Hallegraeff GM, Raven J, Sanders RW, Zubkov M. (2019).

- Sampling bias misrepresents the biogeographic significance of constitutive mixotrophs across global oceans. *Global Ecol. Biogeogr.* **28**: 418–428.
- Leles S, Bruggeman J, Polimene L, Blackford J, Flynn KJ, Mitra A (2021). Differences in physiology explain succession of mixoplankton functional types and affect carbon fluxes in temperate seas. *Prog. Oceanogr.* **190**: 102481.
- Levinsen H, Nielsen TG (2002). The trophic role of marine pelagic ciliates and heterotrophic dinoflagellates in arctic and temperate coastal ecosystems: A cross-latitude comparison. *Limnol. Oceanogr.* **47**: 427–439.
- Levinsen H, Nielsen TG, Hansen BW (2000). Annual succession of marine pelagic protozoans in Disko Bay, West Greenland, with emphasis on winter dynamics. *Mar. Ecol. Prog. Ser.* **206**: 119–134.
- Lynn DH, Montagnes DJS (1991). Global production of heterotrophic marine planktonic ciliates. NATO AS Series, *Protozoa and Their Role in Marine Processes*, **25**: 281–307.
- Lynn DH, Montagnes DJS, Small EB (1988). Taxonomic descriptions of some conspicuous species in the family strombidiidae (Ciliophora: Oligotrichida) from the isles of shoals, gulf of maine. *J. Mar. Biol. Assoc. U.K.* **68**: 259–276.
- Mahé F, Rognes T, Quince C, de Vargas C, Dunthorn M (2014). Swarm: robust and fast clustering method for amplicon-based studies. *PeerJ*. doi:10.7717/peerj.593.
- Martin M (2011) Cutadapt removes adapter sequences from high-throughput sequencing reads. *EMBnet.journal*. doi:10.14806/ej.17.1.200.
- Medlin LK, Kooistra WHCF (2010). Methods to estimate the diversity in the marine photosynthetic protist community with illustrations from case studies: A review. doi:10.3390/d2070973.
- Meire L, Mortensen J, Meire P, Juul-Pedersen T, Sejr MK, Rysgaard S, *et al.* (2017). Marine-terminating glaciers sustain high productivity in Greenland fjords. *Glob. Chang. Biol.* **23**: 5344–5357.
- Menden-Deuer S, Lessard EJ (2000). Carbon to volume relationships for dinoflagellates, diatoms, and other protist plankton. *Limnol Oceanogr* **45**: 569- 579.
- Mitra A, Flynn KJ (2021) HABs and the Mixoplankton Paradigm. *Harmful Algae News* **67**: 4-6.
- Mitra A, Flynn KJ, Burkholder JM, Berge T, Calbet A, Raven JA, Granéli E, Glibert PM, Hansen PJ, Stoecker DK, Thingstad F, Tillmann U, Våge S, Wilken S, Zubkov M (2014). The role of mixotrophic protists in the biological carbon pump. *Biogeosciences* **11**: 995–1005.
- Mitra A, Flynn KJ, Tillmann U, Raven JA, Caron D, Stoecker DK, Not F, Hansen PJ, Hallegraeff G, Sanders RW, Wilken S, McManus G, Johnson MD, Pitta P, Vågen S, Berge T, Calbet A, Thingstad F, Jeong HJ, Burkholder J-A, Glibert PM, Granéli E, Lundgren V (2016). Defining planktonic protist functional groups on mechanisms for

- energy and nutrient acquisition: Incorporation of diverse mixotrophic strategies. *Protist* **167**: 106–120.
- Modigh M (2001). Seasonal variations of photosynthetic ciliates at a Mediterranean coastal site. *Aquatic Micro. Ecol.* **23**: 163–175.
- Montagnes DJS, Lynn DH, Stoecker DK, Small EB (1988). Taxonomic descriptions of one new species and redescription of four species in the family Strombidiidae (Ciliophora, Oligotrichida). *J. Protozoo.* **35**: 189–197.
- Mortelmans J, Deneudt K, Cattrijsse A, Beauchard O, Daveloose I, Vyverman W, *et al.* (2019). Nutrient, pigment, suspended matter and turbidity measurements in the Belgian part of the North Sea. *Sci. Data* **6** : 1–9.
- Passy P, Gypens N, Billen G, Garnier J, Thieu V, Rousseau V, Parent J-Y, Lancelot C (2013). A model reconstruction of riverine nutrient fluxes and eutrophication in the Belgian coastal Zone since 1984. *J. Mar. Sys.* **128** : 106–122.
- Peuto-Moreau M (1991) *Symbiose Plastidiale et Mixotrophie des Ciliés Planctoniques Marins Oligotrichina (Ciliophora)*. Thèse de doctorat d' état, Université de Nice-Sophia Antipolis, Nice.
- Pitta P, Giannakourou A (2000). Planktonic ciliates in the oligotrophic Eastern Mediterranean: Vertical, spatial distribution and mixotrophy. *Mar. Ecol. Prog. Ser.* **194**: 269–282.
- Pitta P, Giannakourou A, Christaki U. (2001). Planktonic ciliates in the oligotrophic Mediterranean Sea: Longitudinal trends of standing stocks, distributions and analysis of food vacuole contents. *Aquat. Micro. Ecol.* **24**: 297–311.
- Porter KG, Feig YS (1980). The use of DAPI for identifying and counting aquatic microfloral. *Limnol. Ocean.* **25**: 943–948.
- Pruesse E, Quast C, Knittel K, Fuchs BM, Ludwig W, Peplies J., *et al.* (2007). SILVA: A comprehensive online resource for quality checked and aligned ribosomal RNA sequence data compatible with ARB. *Nucleic Acids Res.* doi:10.1093/nar/gkm864.
- Putt M (1990). Abundance, chlorophyll content and photosynthetic rates of ciliates in the Nordic Seas during summer. *Deep. Res.* **37**: 1713–1731.
- Putt M, Stoecker DK (1989). An experimentally determined carbon:volume ratio for marine oligotrichous ciliates from estuarine and coastal waters. *Limnol. Oceanogr.* **34**: 1097–1103.
- Richardson K, Nielsen TG, Pedersen FB, Heilmann JP, Løkkegaard B, Kaas H (1998) Spatial heterogeneity in the structure of the planktonic food web in the North Sea. *Mar. Ecol. Prog. Ser.* **168** : 197–211.
- Rognes T, Flouri T, Nichols B, Quince C, Mahé F (2016) VSEARCH: a versatile open source tool for metagenomics. *PeerJ.* doi:10.7717/peerj.2584.

- Romano F, Symiakaki K, Pitta P (2021). Temporal variability of planktonic ciliates in a coastal oligotrophic environment: Mixotrophy, size classes and vertical distribution. *Front. Mar. Sci.* **8**: doi:10.3389/fmars.2021.641589.
- Rousseau V, Becquevort S, Parent JY, Gasparini S, Daro MH, Tackx M, Lancelot C (2000). Trophic efficiency of the planktonic food web in a coastal ecosystem dominated by *Phaeocystis* colonies. *J. Sea Res.* **43**: 357–372.
- Santoferrara LF (2019). Current practice in plankton metabarcoding: Optimization and error management. *J. Plankton Res.* **41**: 571–582.
- Schneider LK, Flynn KJ, Herman PMJ, Troost TA, Stolte W (2020) Exploring the trophic spectrum: placing mixoplankton into marine protist communities of the southern North Sea. *Front. Mar. Sci.* **7**: 586915.
- Simó R (2001). Production of atmospheric sulfur by oceanic plankton: Biogeochemical, ecological and evolutionary links. *Trends Ecol. Evol.* **16**: 287–294.
- Stern R, Kraberg A, Bresnan E, Kooistra WHCF, Lovejoy C, Montresor M, Morán XAG, Not F, Salas R, Siano R, Vaultot D, Amaral-Zettler L, Zingone A, Metfies K (2018). Molecular analyses of protists in long-term observation programmes - Current status and future perspectives. *J. Plankton Res.* **40**: 519–536.
- Stoecker, D. K., Lavrentyev, P. J. (2018). mixotrophic plankton in the polar seas : a pan-arctic review. *Front. Mar. Sci.* **5**: 292
- Stoecker DK, Michaels AE, Davis LH (1987) Large proportion of marine planktonic ciliates found to contain functional chloroplasts. *Nature* **326**: 790–792.
- Stoecker DK, Taniguchi A, Michaels AE (1989). Abundance of autotrophic, mixotrophic and heterotrophic planktonic ciliates in shelf and slope waters. *Mar. Ecol. Prog. Ser.* **50**: 241–254.
- Stoecker DK, Gifford DJ, Putt M (1994). Preservation of marine planktonic ciliates - Losses and cell shrinkage during fixation. *Mar. Ecol. Prog. Ser.* **110**: 293-299.
- Stoecker DK, Johnson MD, De Vargas C, Not F (2009). Acquired phototrophy in aquatic protists. *Aquat. Microb. Ecol.* **57**: 279–310.
- Stolte W, Riegman R (1995). Effect of phytoplankton cell size on transient-state nitrate and ammonium uptake kinetics. *Microbiology* **141**: 1221–1229.
- Strickland J, Parsons T (1972) *A practical handbook of seawater analysis*. Edn Ottawa, CA: Fisheries Research Board of Canada.
- Szeligowska M, Trudnowska E, Boehnke R, Dąbrowska AM, Dragańska-Deja K, Deja K, Dareckic M, Błachowiak-Samołyka K (2021). The interplay between plankton and particles in the Isfjorden waters influenced by marine- and land-terminating glaciers. *Sci. Total Environ.* **780**. doi:10.1016/j.scitotenv.2021.146491.
- Tong M, Smith JL, Kulis DM, Anderson DM (2015). Role of dissolved nitrate and phosphate in isolates of *Mesodinium rubrum* and toxin-producing *Dinophysis acuminata*. *Aquat. Microb. Ecol.* **75**: 169–185.

- Utermöhl H (1931). Neue Wege in der quantitativen Erfassung des Plankton (Mit besonderer Berücksichtigung des Ultraplanktons.). SIL Proceedings, 1922-2010. <https://doi.org/10.1080/03680770.1931.11898492>
- Utermöhl H (1958) Zur Vervollkommnung der quantitativen Phytoplankton-Methodik. SIL Commun. 1953-1996 9, 1–38. doi:10.1080/05384680.1958.11904091.
- van Leeuwen S, Tett P, Mills D, van der Molen J (2015), Stratified and nonstratified areas in the North Sea: Long-term variability and biological and policy implications, *J. Geophys. Res. Oceans* **120**: 4670–4686,
- Zubkov MV, Tarran GA (2008). High bacterivory by the smallest phytoplankton in the North Atlantic Ocean. *Nature* **455**: 224-226.